ChemComm

Unconventional Conjugation in macromonomers and polymers.

Journal:	*ChemComm*
Manuscript ID	CC-FEA-07-2022-003968.R2
Article Type:	Feature Article

Unconventional Conjugation in macromonomers and polymers.

Richard M. Laine
Dept. of Materials Science and Engineering
University of Michigan
Ann Arbor, MI 48109-2136
talsdad@umich.edu

Abstract

Multiple reviews have been written concerning conjugated macromonomers and polymers both as general descriptions and for specific applications. In most examples, conjugation occurs via electronic communication via continuous overlap of π orbitals most often on carbon. These systems can be considered to offer traditional forms of conjugation. In this review, we attempt to survey macromonomers and polymers that offer conjugation involving novel forms of carbon and/or other elements but with conjugation achieved via other bonding formats including many where the mechanism(s) whereby such behavior is observed remain unresolved.

In particular, this review emphasizes silsesquioxane containing polymeric materials that offer properties found typically in conjugated polymers. However, conjugation in these polymers appears to occur via saturated siloxane bonds within monomeric units that make up a variety of polymer systems. Multiple photophysical analytical methods are used as a means to demonstrate conjugation in systems where traditional conjugation is not apparent.

Introduction

Research on conjugated polymers has experienced exceptional growth over the last 60+ years[1,2] as multiple types of organic polymers have been identified that exhibit through chain conjugation coincident with offering utility in diverse applications arising from commercially useful photonic,[3–6] electronic,[7,8] sensor,[9,10] energy storage,[11] and bio-medical[12] properties to name several. Coincident with this growth, one can also find extensive studies targeting the development of new synthetic approaches to conjugated systems.[13–15]

Our goal in this review is not to rehash the extensive literature on conjugated polymer synthesis, structure-property relationships or applications but rather to highlight systems that exhibit what might be defined as unconventional conjugation. Thus, to begin with, it is expedient that we first provide a working definition of conjugation.

Defining conjugation.

The general concept of conjugation in organic chemistry is often explained as electronic communication between π-orbitals on adjacent atoms that allows charge delocalization across atom chains such that the overall energy of the polymer (macromonomer) of interest is reduced by approximately the same energy as the π* antibonding orbitals increases and is typically chain length dependent. Traditional examples of this nature would include polyacetylenes,[16–19] polyanilines,[20–23] polythiophenes,[24–27] and polypyrroles.[28–31] It is important to recognize that these polymer systems offer properties that vary from insulating to semiconducting to metallic. Furthermore, these properties are relatively amenable to modification often via simple synthetic methods allowing great scope in terms of manipulation for property specific applications.

Less traditional systems would include non-carbon atoms in the main chain especially those that form double bonds and can participate in π-π conjugation including polymers with nitrogen and phosphorus introduced to traditionally conjugated polymers.[32–35] While these latter systems are interesting in their own right for example because they can bind metals to the polymer backbone and also offer n-π* transitions in addition to π-π* absorption and emission behavior, they do not offer unconventional (unexpected) conjugation.

In keeping with subsets of polymers with non-carbon atoms in the main chain, it is important to call attention to sets of polymers with metal atoms and alkynes in the main chain that was recently reviewed.[36–39] Again, these systems do not exhibit properties indicative of unconventional conjugation. In the cited platinum acetylide papers, it is posited that some dπ-pπ conjugation may occur. However, an alternate explanation offered suggests there may be exciton interactions between the organic moieties.

As an outlier, the non-carbon polythiazyl or -$(S{=}N)_x$-[40–43] is one of a few limited examples where conjugation does not involve carbon. However, the mechanism whereby SN_x exhibits conjugation to the point where it offers metal-like (even super) conductivities remains vague and poorly explored and may not be via π-π conjugation.[44,45]As such attempts to provide more details on its conjugation without sufficient background are not appropriate.

At this point, one might choose to expand this definition to materials that exhibit conjugation defined by electronic delocalization of charge across multiple atoms within a molecular structure as evidenced by red-shifts in absorption and/or emission vs smaller analogs of the same approximate structure. This latter definition can encompass clusters of atoms that may or may not have π bonds but still offer delocalization as we will discuss below including carbon nanodots, carboranes, polyatomic metal clusters and silsesquioxanes.

Carbon based materials.

It is first important to also discuss limitations beginning with a discussion of what is the boundary between molecular and nanostructured behavior or what distinguishes a bulk material from a cluster, macromonomer, oligomer or polymer?

For our purposes, it is valuable to first consider materials close to bulk carbon. Amorphous carbon, consisting of a 3-D mixture of sp^2 and sp^3 hybridized bonds with sufficient numbers of the former to offer 3-D conductivity, can be defined as a bulk material and thus not part of our discussion.

Unlike amorphous carbon, graphite consists of planes of sp^2 hybridized carbon (graphite plane = graphene) that provide electron and phonon delocalization via π-π interactions within a given plane but much less across planes. One can suggest that graphite is also a bulk material and is therefore also not considered here. In contrast, single and double layer graphenes offer two-dimensional regularity with extended π-π conjugation as found in conjugated polymers. However, for our objectives they offer conventional conjugation and can be regarded as materials rather than polymers. Conjugation in graphenes has been addressed in reviews.[46–48]

However, graphenes have been compared to polycyclic aromatic hydrocarbons and one might choose to consider graphene nanodots as graphene segments making the leap from material to macromolecular somewhat indistinct.[47] Graphene dots then can be used as the boundary between conjugated materials and conjugated polymers structures if we consider nanodots as 2-D macromolecules that exhibit behavior best described in analogy to well-defined conjugated polymers.

Carbon nanodots can offer quantum confined behavior meaning they exhibit absorption and emission behavior where the relaxed excitonic radius is greater than the diameter of the particle. This has the effect of driving the exciton energies higher than found in the relaxed stated such that particle sizes below the relaxed excitonic radius control the absorption and emission wavelengths (energies). Again, the operative question here is when does the dot become small enough that it looks like a macromonomer. Answering this question is beyond the scope of this review. We briefly address the properties of these materials just below despite the obvious conundrum.

Carbon nanodots (CDs)

There are already multiple reviews on carbon nanodots typically recognized to be particles < 10 nm in diameter.[49–51] Our concern here is if they demonstrate unconventional conjugation and then whether it is molecular or nanostructured. In general, CDs contain large numbers of sp^2 carbons implying π-π conjugation;[52,53] however, arguments are made that emissive behavior is size dependent implying quantum confinement. This would then not be of interest to this review. But, there are examples where decreasing size leads to red rather than blue shifts; contrary to quantum confinement. Furthermore, high emissive quantum efficiencies can be directly correlated with surface functionalization/passivation. This leads to conclusions that surface states may be responsible for emissive behavior for some CDs *which may imply* novel forms of conjugation.

One explanation for this is that photoexcitation typically occurs nearer CD cores which are often found to be more crystalline. Thereafter, energy is transferred to surface emissive states or even appended organics.[54] The question to be answered is whether energy transfer is by conjugation or charge transfer. In addition, it has been reported that multiple emissions can arise simultaneously which may reflect different surface defects responsible for exciton emission

and/or different emitting moieties or different conjugation pathways or all three. The latter may reflect unconventional conjugation.

With respect to this last possibility, two further points to make concern the observation of excitation dependent emissions contrary to Kasha's rule;[54,55] which states that no matter what the excitation wavelength, lowest energy excited state will be the emitting state. One simple explanation may be that the excitation wavelength dependent emission wavelengths for CDs may simply be a consequence of the presence of impurities.[56,57] In addition, and perhaps associated with these phenomena are the fact that carbon nanodots are also known to upconvert light (two lower energy photons to one higher energy photons) and also offer two photon absorption cross-sections (TPA) that can be very much higher than traditional organic molecules.[58] These observations may be used to argue unconventional conjugation.

The TPA data is mentioned because it may be a mechanism for identifying unconventional conjugation that is not an artifact of impurities, or surface states as we discuss below in developing some concepts for silsesquioxane macromonomer and polymer photophysical behavior. Again, CD based materials await further clarification of the issues noted.

We can now begin to move away from pure carbon-based materials to well-defined carborane clusters that can be clearly called molecular structures.

Carboranes

Can be defined as polyhedral clusters of carbon and boron typically capped with hydrogen which provides points for appending other functional groups, Figure **1**.[59,60] Related structures can have one or two vertices missing are called *nido*- or *arachno*-carboranes respectively. There is at least one example of a "flat carborane."[61] Many more structures have been described but are not relevant to the topic. If one considers aromaticity as a subset of conjugation then there are multiple examples wherein carboranes exhibit aromaticity, as recently reviewed by Jäkle.[62] The source of aromaticity in carboranes has been discussed in terms of available electrons delocalized between carbons and boron in π, empty p bonds on boron, and σ bonds within the carborane.[61,62]

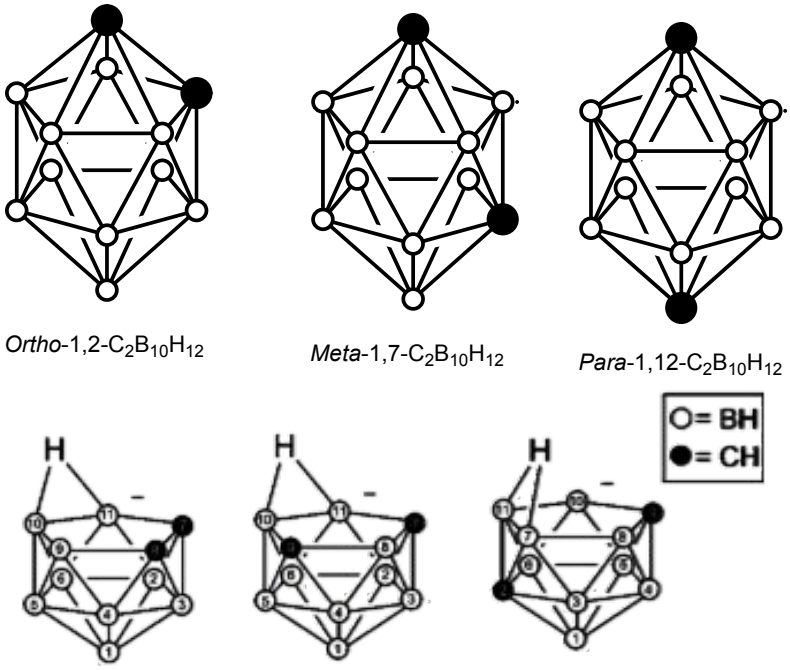

nido-7,8-$C_2B_9H_{12}^-$, *nido*-7,9-$C_2B_9H_{12}^-$, *nido*-2,9-$C_2B_7H_{13}$

Figure 1. Examples of well-known carborane structures [Reproduced from ref. 63 with permission from American Chemical Society, 2011].[63]

Cook et al[60] have synthesized carborane oligomers finding a form of conjugation they suggest arises from radical anion electron transfer between the Figure **2** *p*-carborane cages, finding that the radical anions are fully delocalized across the phenyls and p-carborane. These results indicate delocalization that can be ascribed to Robin−Day class III intervalent (OET) transition states revealing that *p*-carboranes promote conjugation.

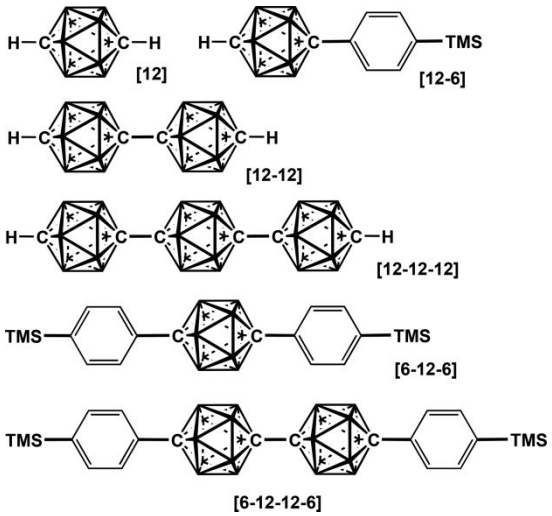

Figure 2. Examples of carborane oligomers [Reproduced from ref. 60 with permission from American Chemical Society, 2018].[60]

In contrast to the Cook work, a number of groups have synthesized polymers with carboranes in their main chain that offer extended conjugation that must directly involve the carborane cluster as pioneered by the Chujo group.

The Chujo group first described several examples of simple, organic modified carboranes that exhibit conjugation in the form of modified luminescent behavior (Figure **3**).[64–67] Thereafter, they synthesized a series of *m*-carborane copolymers (Figure **4)** that clearly show conjugation with photophysical properties (emissive/color) that vary with the comonomer.[64,65,67]

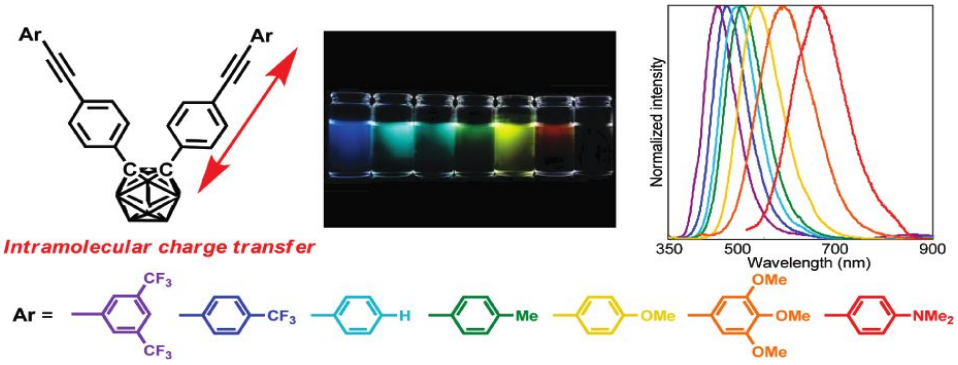

Figure 3. Alkyne appended orthocarborane [[Reproduced from ref. 67 with permission from American Chemical Society, 2011].[67]

Thereafter they succeeded in synthesizing polymeric systems with boron in the main chain via hydroboration and then discovered halo-phenyl boronation, Figure **5**. In the latter systems, conjugation is suggested to occur via π-empy *p* orbital on the boron.

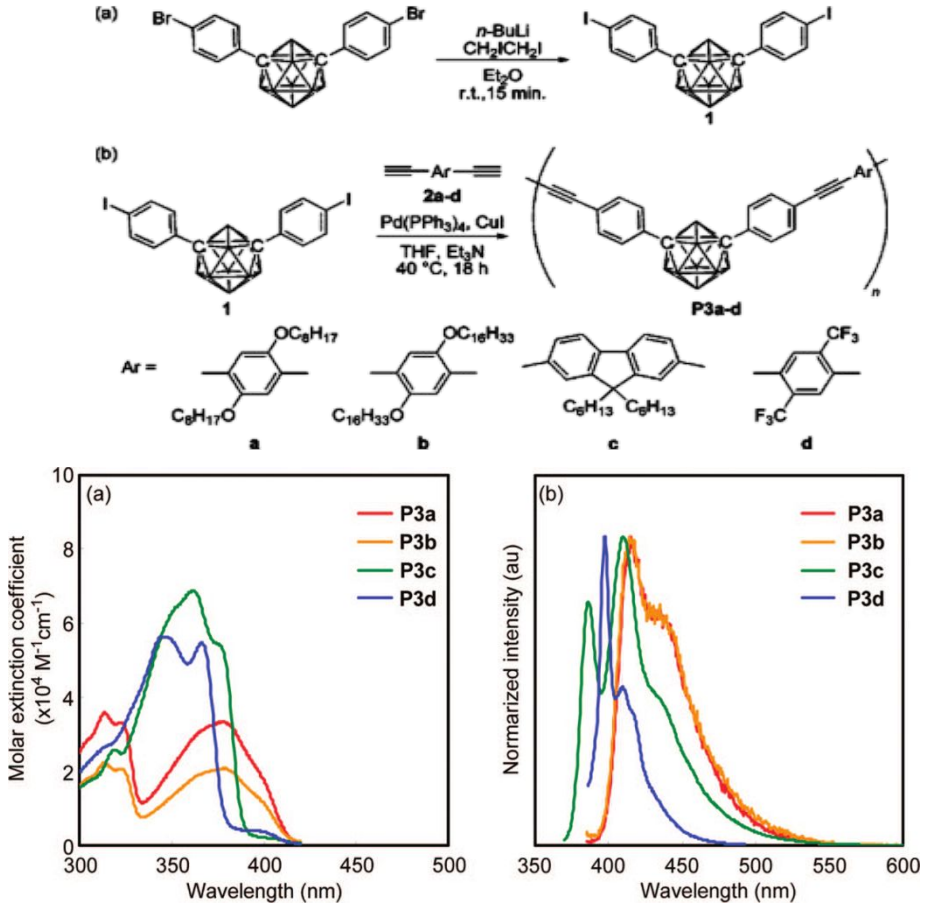

compound	λ_{max} (nm)[a]	$\varepsilon\lambda_{max}$ (M^{-1} cm^{-1})[a]	Ex (nm)[b,c]	PL (nm)[c]	Stokes shift (nm)[c]	Φ_F[d]
P3a	314, 378	36 000	378	415	37	0.25
P3b	314, 378	22 000	378	415	37	0.25
P3c	319, 362	69 000	362	386, 410	24, 38	0.11
P3d	345, 366	56 400	366	409	43	0.22
6	313, 375	33 000	375	414	39	0.23
7	307, 365	41 000	365	403	38	0.49

[a] Measured in $CHCl_3$ (1.0×10^{-5} M) at room temperature. [b] Excited wavelength. [c] Measured in $CHCl_3$ (1.0×10^{-7} M). [d] Fluorescence quantum yields (relative to 9,10-diphenylanthracene in cyclohexane at room temperature).

Figure 4. Copolymers of bis(*p*-bromophenyl *m*-Carborane) with various p-aromatic dialkynes [Reproduced from ref. 64 with permission from American Chemical Society, 2009].[64]

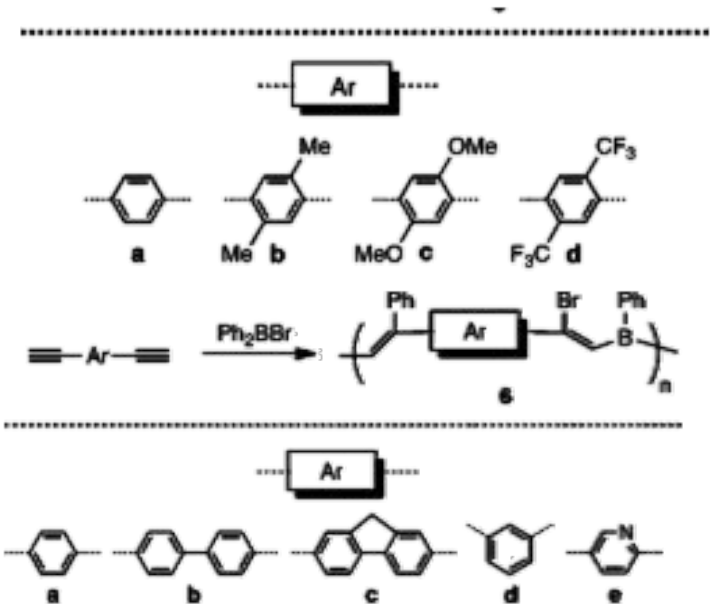

Figure 5. General synthetic routes to alkenyl and bromoalkenyl polyboranes [Reproduced from ref. 62 with permission from American Chemical Society, 2010].[62]

Ferrocene functionalized *o*-carborane monomers and aromatic bridged dimers (Figure **6**) have been synthesized and their electrochemistry and photophysical properties reported.[68] In general, evidence is presented that the carborane unit affects both the HOMO and the LUMO as evidenced by shifts in the absorption wavelengths and changes in the cyclic voltametric traces (redox behavior) of the ferrocenyl moieties.

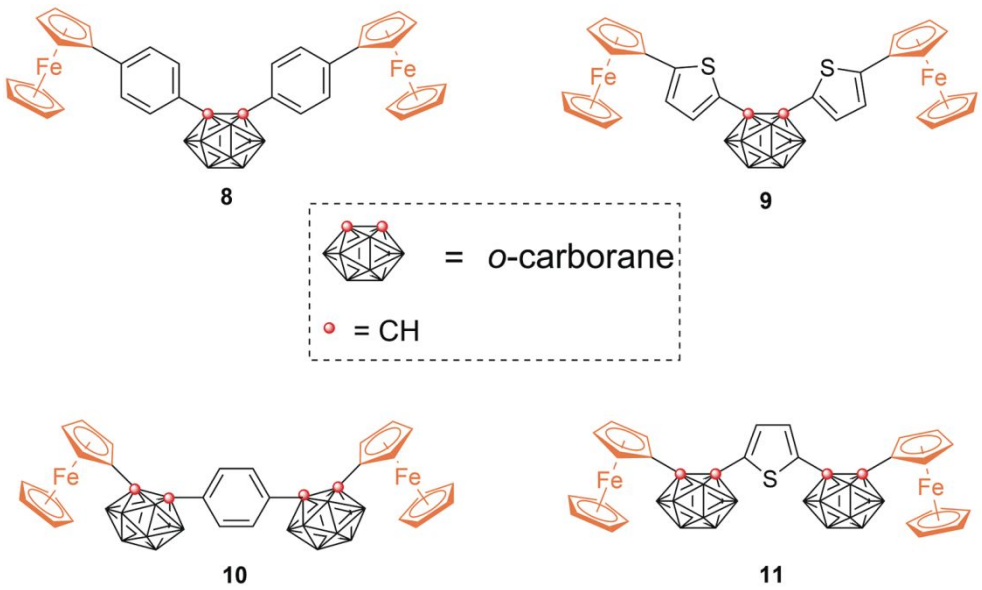

Figure 6. Oligomers of *o*-carborane bonded to ferrocene and selected aromatic bridging systems [[Reproduced from ref. 68 with permission from Royal Chemical Society, 2020].[68]

Unfortunately, no examples of longer chains are given that might offer further evidence for through carborane conjugation inclusive of the ferrocene units. For a more detailed discussion of boron containing polymers that show conjugation, the reader is referred to the Jäkle review.[62]

Non-carbon clusters.

Work by the Sevov group on metal cluster compounds[69] may be viewed as strictly inorganic chemistry; however, DFT calculations on the Figure **7** Ge cluster compound suggest π-π delocalization via p_z bonds such that all four Ge clusters are conjugated making this one of the more exotic systems showing unconventional conjugation.

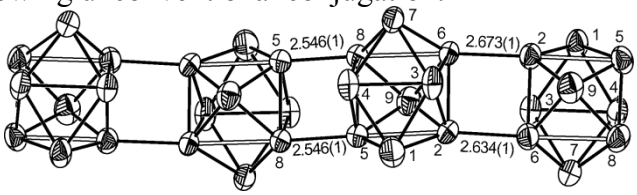

Figure 7. $(Rb\text{-}18C6)_8[Ge_9{=}Ge_9{=}Ge_9{=}Ge_9]{\cdot}2en$ 18C6 is crown ether and en is ethylene diamine [Reproduced from ref. 69 with permission from American Chemical Society, 2003].[69]

In related work on Sn clusters (Figure **8**),[70] the same group reports that the pentagonal rings in these columnar clusters also resemble cyclopentadienides and exhibit what is classified as conjugation within the rings. In addition, because these compounds offer conducting behavior based on the availability of two extra electrons, indicates that these systems are conjugated via what is suggested to be overlapping cationic *s*-orbitals and π^*-orbitals on the Sn_5^{6-} cyclomers suggesting that communication occurs along and between the stacks.

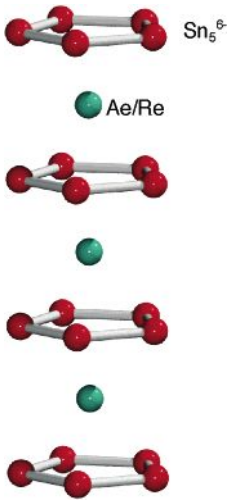

Figure **8**. Stacked Sn_5^{6-} aromatic rings separated by Ca/Eu (AeRe) cations [Reproduced from ref. 70 with permission from American Chemical Society, 2005].[70]

A further example from the same publication shows a polymer like structure, Figure **9**, which is suggested to offer conjugation reminiscent of polyacetylene.

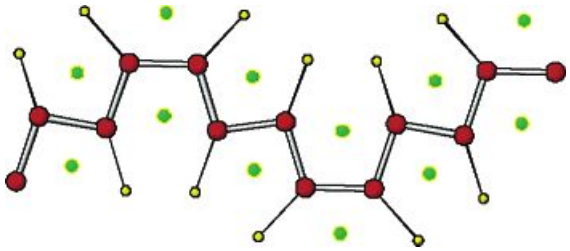

Figure 9. Fragment of flat zigzag chain in $LiMg(Eu/Sr)_2Sn_3$ with coplanar Li/Mg mixed occupancy positions (M), resembling a polyacetylene, $(CH)_\infty$. Chain. Eu/Sr = light-green spheres above and below plane of chain [Reproduced from ref. 70 with permission from American Chemical Society, 2005].[70]

Unfortunately, these systems are highly air and moisture sensitive complicating any efforts to explore modification via appended conjugated organic groups. If this were at all possible, it might provide hybrid systems perhaps also providing a stabilizing effect, making them more attractive for further studies.

Gold and Silver clusters are well-known and studied in great detail especially with respect to their quantum dot-like behavior and ability to exhibit electron delocalization.[71–74] This subject area deserves a review in its own right and cannot be addressed here.

While we have touched on the structures of metal clusters with the work of Sevov et al, it is clear that there are numerous other metal cluster systems that could also be mentioned and it is the authors decision that this constitutes too large and diverse a subject area to address given our original mission which focuses on silicon containing systems.

Unconventional conjugation in silsesquioxanes (SQs)

SQs offer multiple unique properties including well defined 3-D nanostructures with regular symmetry; cubic for T_8 $[(RSiO_{1.5})_8]$, D_{5h} for T_{10} $[(RSiO_{1.5})_{10}]$ and C_{2V} for T_{12} $[(RSiO_{1.5})_{12}]$ cages. The single crystal silica-like cores suggests that SQs are simply organic decorated silica nanoparticles imbuing extremely robust properties to any derivatives synthesized therefrom such that selected polyamides offer thermal stabilities in air to 600 °C.[75–79]

Additionally, they can be multiply and selectively functionalized in 3-D at 1-3 nm length scales, particularly the phenyl and vinyl derivatives, using a wide variety of chemical reactions but especially electrophilic substitutions to introduce multiple moieties at their peripheries.[80] Figure **10** provides examples of the types of SQ (R-$SiO_{1.5}$) and Q (O-$SiO_{1.5}$) cages known in the literature. Hence they have been extensively studied for their structural properties and multiple reviews and one book have appeared in the last 30$^+$ years.[81–96]

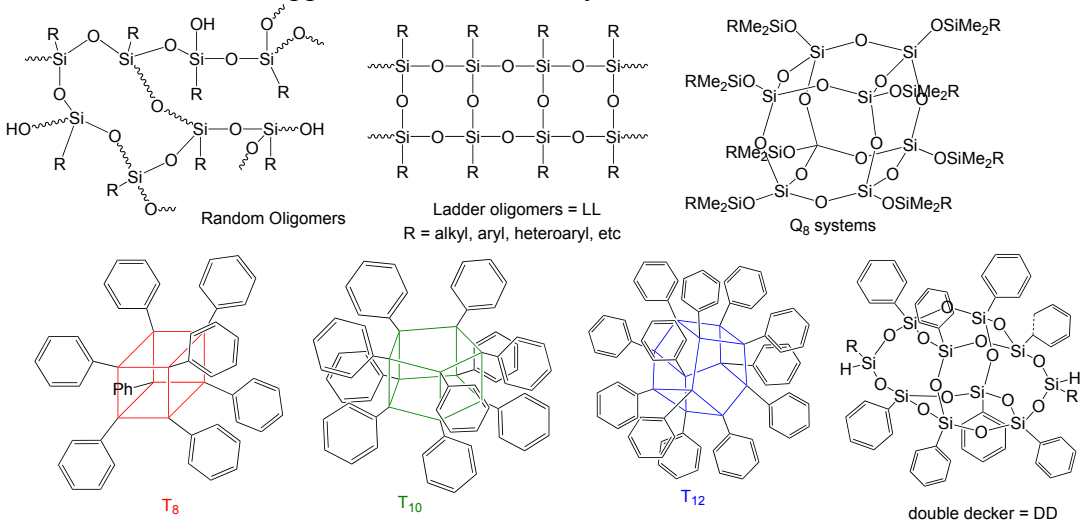

Figure 10. Examples of various T ($RSiO_3$) and Q (SiO_4) cages.

Our original interest in these compounds extends from their high symmetry and approximately one nanometer diameters as potential nanobuilding blocks, especially the octaphenyl silsesquioxane, $[PhSiO_{1.5}]_8$, OPS. With cubic symmetry, OPS places each phenyl in a different octant in Cartesian space in principle offering the potential construct 3-D connected structures nanometer by nanometer. Efforts to functionalize OPS led to the discovery that this compound can be nitrated in fuming nitric acid to give the *m*-octanitro compound that is readily reduced to the octaaminophenyl compound.[97] This finding suggested exploring electrophilic substitution reactions leading to studies on bromination and iodination.[98–100]

Initial bromination studies used an iron catalyst resulting in product distributions recorded in Table **1**. By accident, a bromination reaction was run without adding iron with the extremely surprising finding that bromination proceeds almost exclusively at the *ortho* position. Equally surprising is iodination with ICl gives primarily *p*-I_8OPS.[100] Likewise, bromination of $[PhSiO_{1.5}]_{10,12}$ without catalyst also preferentially goes *ortho* and ICl gives para iodination.[100,101]

Table 1. Bromination and iodination of $[PhSiO_{1.5}]_8$ with/without Fe catalysis [Reproduced from ref. 98 with permission from American Chemical Society, 2005].[98,101]

$Br_{5.3}$OPS/Fe catalyzed[98]		Br_8OPS/uncatalyzed[101]	I_8OPS/ICl/0 °C[100]
Major Isomers	Mol Fraction %	Mol Fraction %	
4-halogenation	39	5	95
phenyl	37	2	1-2

3-halogenation	15	5	2-3
2-halogenation	6	85	1
dibrominated	3	3	

Theoretical modeling studies of bromination sans Fe catalyst, reveals the presence of cage centered LUMOs (Figure **11**) for all cages.[102] Apparently the LUMO engages incoming Br_2 presumably extracting electron density. Coincidentally phenyl ortho hydrogens form electrostatic bonds to the incoming Br_2, Figure **12**.

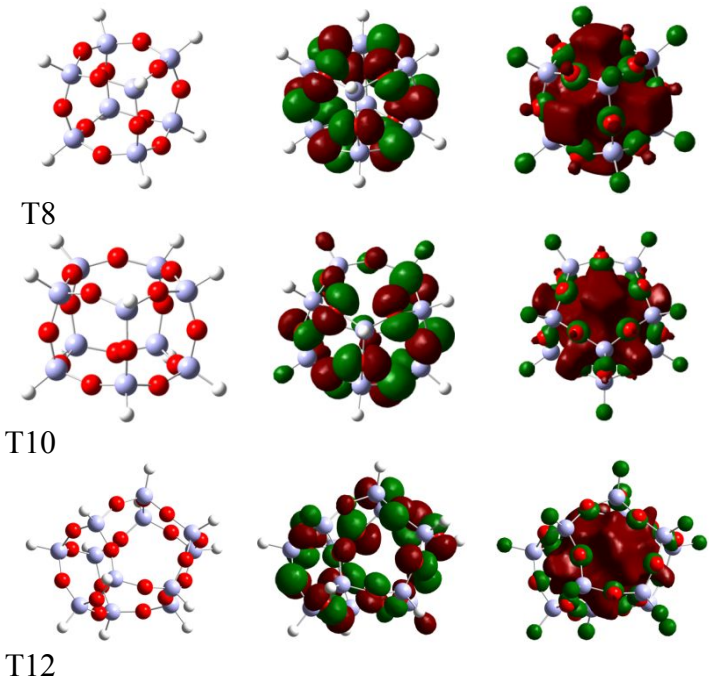

Figure 11. Molecular structures and electron density isocontours of $[PhSiO_{1.5}]_{8,10,12}$. The left column shows a 3D view of the optimized structures with H (white), O (red) and Si (gray). HOMOs are shown in the middle and the right column presents LUMOs [Reproduced from ref. 102 with permission from Royal Chemical Society, 2014].[102]

Efforts to model iodination were unsuccessful. It seems likely that iodine's much larger diameter hinders interactions via the cage face. Thus, *para* substitution is favored despite the likely existence of an energetically accessible LUMO. These results are presented to provide a basis for the reader to understand the photophysical data and explanations of conjugation presented in the following sections.

The opportunity to have well defined and easily purified $[o\text{-}BrPhSiO_{1.5}]_8$ and $[p\text{-}IPhSiO_{1.5}]_8$ provided the impetus for their use as starting points to synthesize nanostructured materials[79,103]

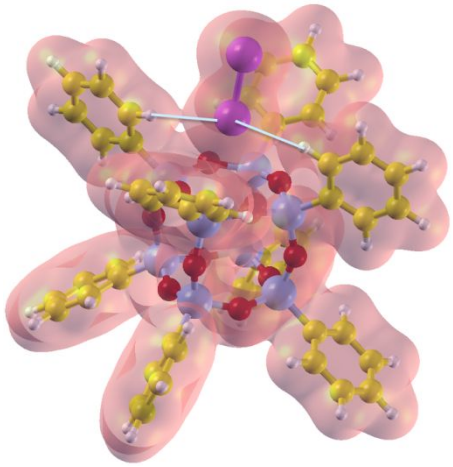

Figure 12. Br_2 absorption centrally above the T_8 cage face is preferred. The face has two phenyls oriented with hydrogens in (wing) and two turned at 90°. Br_2 is stabilized in this configuration by hydrogen bonding to the closer Br atom and the two *o*-hydrogens on the wing-oriented phenyls. Polarization occurs coincidentally as the Br_2 interacts with the T_8 face [Reproduced from ref. 102 with permission from Royal Chemical Society, 2014].[102]

as well as model compounds for photophysical studies. In this latter instance, we began by synthesizing *o*- and *p*-4-substituted stilbenes as models for the eventual synthesis of star versions of polyphenylene vinylene. Although polyphenylene vinylene is a highly efficient blue emitter for display applications;[104,105] its very regular structure means efficient crystal packing leading to very poor solubility thereby making processing difficult.

One can envision that a 3-D analog would offer better solubility and therefore processing of value for display applications. Photophysical characterization of the 4-Rstilbene model compounds unearthed unusual photophysical behavior that completely sidetracked efforts towards these original goals. Heck catalyzed cross coupling of *p*-I_8OPS with 4-substituted styrene provides access to cage appended 4-Rstilbenes.[106] As seen in Figure **13**; all compounds exhibit absorption spectra (320 nm excitation) as expected for simple 4-Rstilbenes $\lambda_{max} \approx$ 280-320 nm. However, all emission λ_{max} are red-shifted ≈ 50-70 nm vs. stilbene and 30-40 nm from the model compound *p*-stilbeneSi(OEt)$_3$. Similar behavior was found for *o*-4Rstilbene analogs.

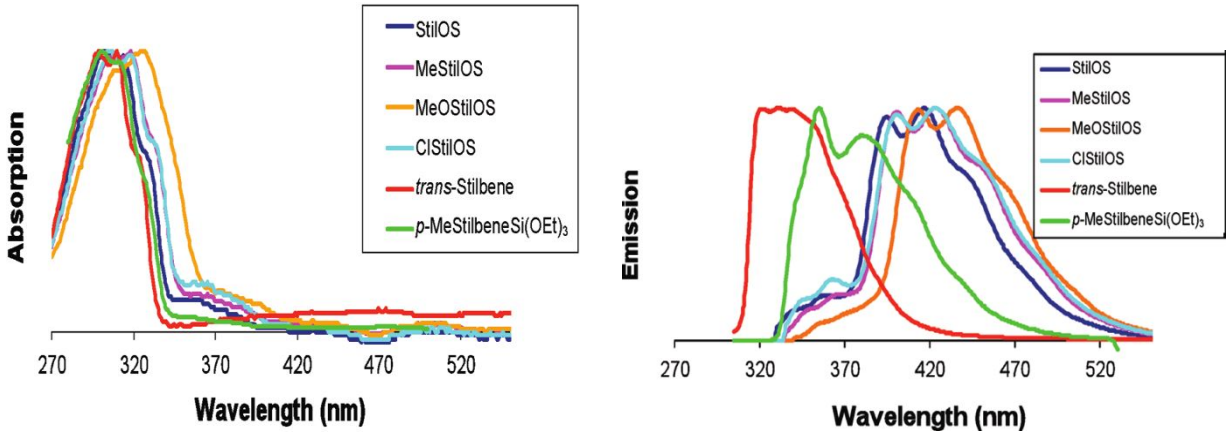

Figure 13a. Normalized absorption. **b**. Emission of [(*p*-4-R-stilbene)$SiO_{1.5}$]$_8$ in THF [Reproduced from ref. 106 with permission from American Chemical Society, 2010].[106]

Traditional interpretation of red-shifts in macromonomers and polymers would indicate greater conjugation lengths thereby reducing π-π* band gaps. One might explain the red-shifts in the *ortho* stilbenes as being a result of formation of internal exciplexes but this cannot work for the *para* derivatives as each appended moiety sits in its own octant in Cartesian space. The only other explanation is conjugation into the cage LUMO in the excited state. Such conjugation is not accessible in the ground state; hence, the lack of coincident ground state red-shifts. Otherwise, fluorescence quantum efficiencies are all < 10 % implying excited states similar to simple stilbenes. This then is the first example of unconventional conjugation in silsesquioxanes.

Coincident with this discovery, was the appearance of work by Bassindale et al and others of a series of SQ cages with encapsulated F^-, Figure **14**.[107,108] One rationale for the formation and stability of these types of structures is the presence of a cage centered LUMO.

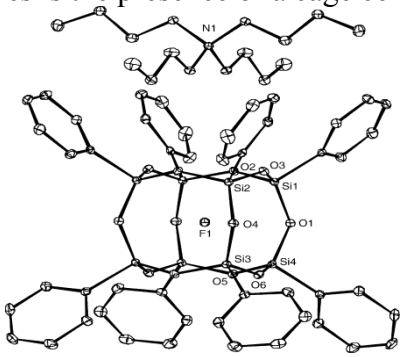

Figure 14. OPS with an encapsulated F^- [Reproduced from ref. 107 with permission from Wiley, 2003].[107]

Complementary evidence in favor of conjugation via cage centered LUMOs comes from finding similar red-shifts obtained by functionalizing $[vinylSiO_{1.5}]_8$ first forming $[4\text{-}BrStryenylSiO_{1.5}]_8$ via metathesis then 4-Rvinylstilbene compounds per Figure **15**.[109] Absorption and red-shifted (vs. vinylstilbene) emission data are shown in Figure **16**. Of particular importance, the Figure **17** absorption and emission behavior of amine terminated NSOVS exhibits a further red-shift in more polar acetonitrile vs CH_2Cl_2. This observation suggests the emitting state results from charge transfer from the NH_2 to the cage centered LUMO, again supporting conjugation.

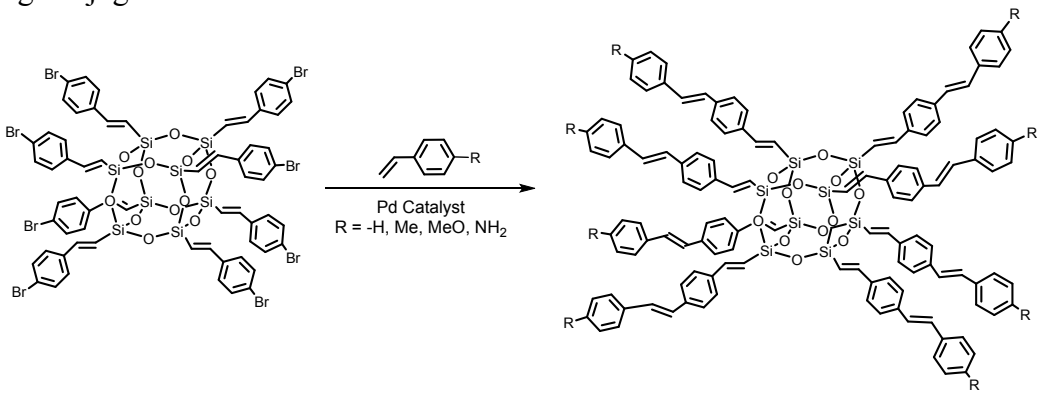

Figure 15. R = -H (SOVS), (*p*-Me) MSOVS, *p*-MeO (OSOVS, *p*-NH_2 (NSOVS) [Reproduced from ref. 109 with permission from American Chemical Society, 2008].[109]

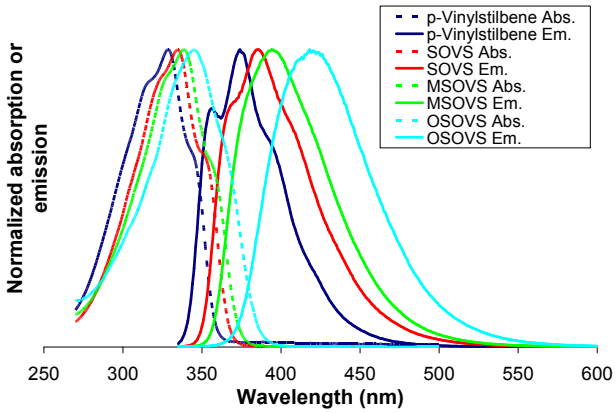

Figure 16. UV-Vis and PL spectra of R-vinylstilbeneOS in THF [Reproduced from ref. 109 with permission from American Chemical Society, 2008].[109]

These results are particularly important when compared with studies on the dimethylaminostilbene substituted compounds shown in Figure **18**. As a mechanism to further characterize these systems, we also conducted two photon absorption (TPA) studies on this series of compounds. TPA cross-sections depend on the degree of polarization of the moieties following absorption of the first photon. Higher polarization coupled with increased stabilization of this state leads to higher measured TPA cross-sections.

Representative two photon absorption (TPA) cross-section studies compare the 4-dimethylaminophenyl compounds of Figure **18** in Figure **19**.[106] The wavelength dependent data plotted reveal very different TPA cross-sections for the full cage vs. the corner and half cages. Table **2** compares TPA data for both systems.

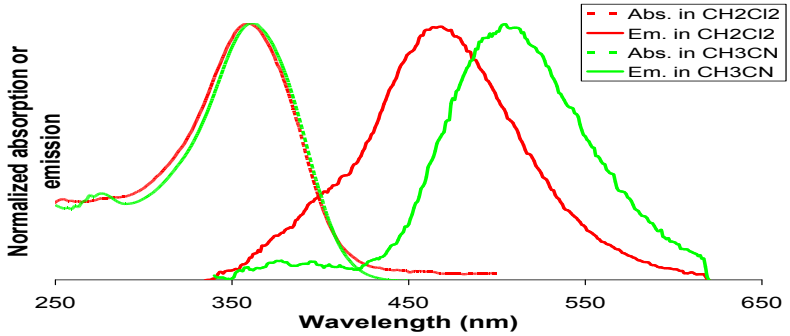

Figure 17. UV-Vis and emission data for NSOVS in two good solvents [[Reproduced from ref. 110 with permission from American Chemical Society, 2008].[110]

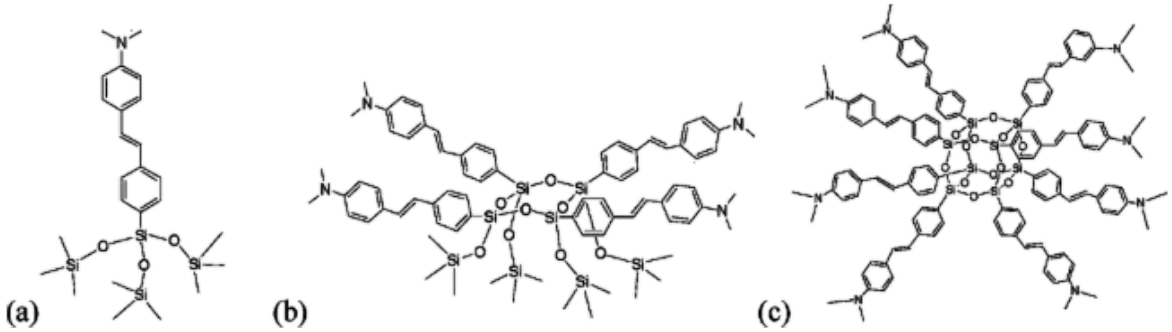

Figure 18. (a) Me_2NStil-corner, (b) Me_2NStil-half, and (c) $[Me_2NStilSiO_{1.5}]_8$ [[Reproduced from ref. 106 with permission from American Chemical Society, 2010].[106]

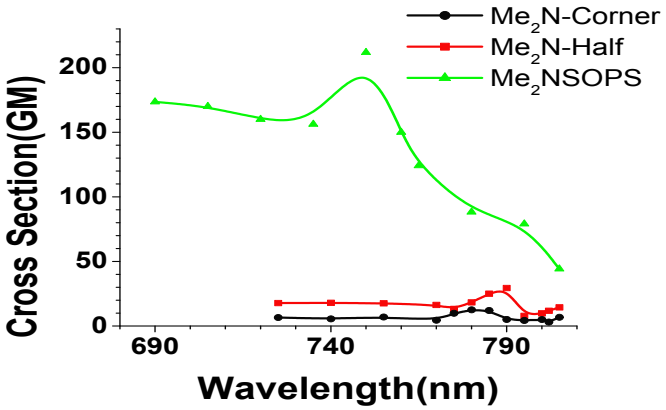

Figure 19. Two-photon absorption cross-section spectra for the investigated chromophores [Reproduced from ref. 106 with permission from American Chemical Society, 2010].[106]

Table 2. TPA properties of silsesquioxane derivatives [Reproduced from ref. 106 with permission from American Chemical Society, 2010][106]

Sample	δ (GM)	δ/moiety (GM)	λ_{max} nm
$MeStil_8OS$	11	1.2	735
Me_2NStil-corner	12	12	780
Me_2NStil-half	30	7.5	790
Me_2NStil_8OS	211	26	755
StilOVS[109]	25	3	705
MeOStilOVS[109]	110	14	705
NH_2StilOVS[109]	810	101	720

One might expect linear behavior for the TPA cross-sections for the Figure **18** compounds but instead (δ GM) values for the full cage are 26/moiety, 8/moiety for the half cage and 12/moiety for the corner. The fact that the full cage offers 2-3 times the TPA of the fragments suggests that this system offers much higher charge transfer than the fragments. The data continue to support the idea of unconventional conjugation via cage centered LUMOs.

The formation of cage encapsulated F^- led to the question of how does the encapsulation process work. To this end, we discovered that F^- can cause extensive cage rearrangements even to the point of promoting depolymerization of cured silicone rubber forming $R_xPh_{8\text{-}1,10\text{-}x,12\text{-}x}$ cages.[111–113] Initial studies explored using F^- to promote synthesis of difunctionalized cages per Figure **18**. Thereafter further functionalized per Figure **19** and then copolymerization per Figure **20**

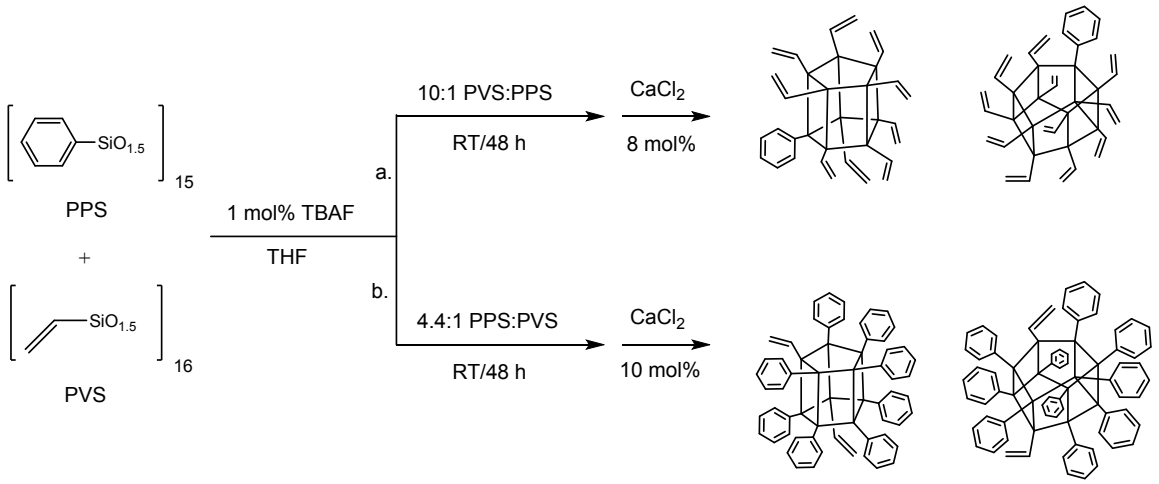

Figure 20. Fluoride-mediated rearrangement of PPS and PVS to (a) $vinyl_xPh_1$ (x = 9, 11) T_{10} and T_{12} and (b) $vinyl_2Ph_x$ (x = 8, 10) T_{10} and T_{12} silsesquioxanes [Reproduced from ref. 111 with permission from American Chemical Society, 2010].[111]

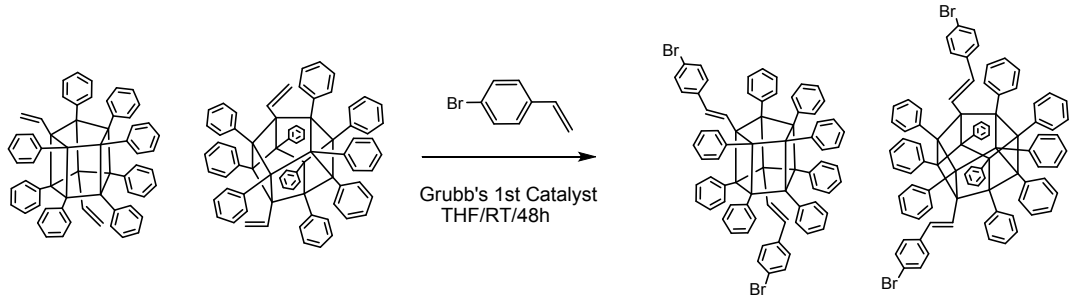

Figure 21. Alkene metathesis of $vinyl_2Ph_x$ (x = 8, 10) T_{10} and T_{12} SQs with 4-bromostyrene [Reproduced from ref. 111 with permission from American Chemical Society, 2010].[111]

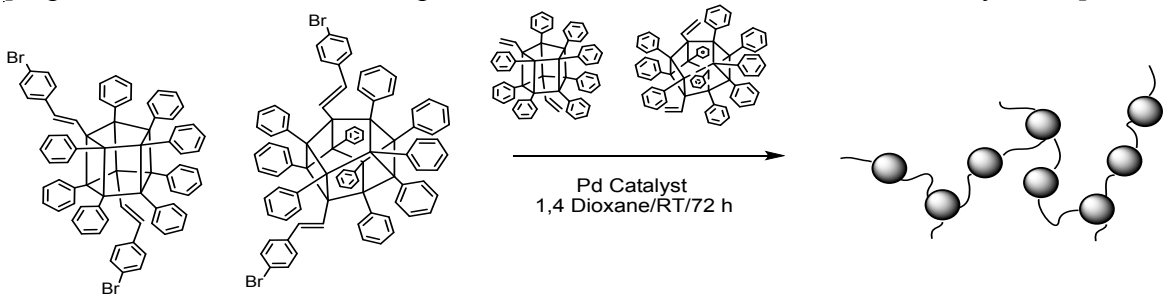

Figure 22. Heck coupling $vinyl_2Ph_x$ T_{10}/T_{12} SQs with $BrStyr_2Ph_x$ T_{10}/T_{12} SQs (x = 8, 10) [Reproduced from ref. 111 with permission from American Chemical Society, 2010].[111]

provides oligomers joined by divinylbenzene tethers. Model single cages with divinylbenzene endcapped with triethoxysilyl groups were also synthesized and the photophysical properties of both systems compared as seen in Figure **25**.

In the Figure **23** spectra, the model compounds absorb ($\lambda_{max} \approx 255$ nm) and emit ($\lambda_{max} \approx 325$ nm) as expected for divinylbenzene alone. The oligomers absorb at the same energies ($\lambda_{max} \approx 255$ nm) but in contrast present red-shifted emissions ($\lambda_{max} \approx 385$ nm). Given the above explanations of the source of these red-shifts, we can suggest that these "beads on a chain" or BoCs exhibit conjugation both via the divinylbenzene tethers and via the T_{10} and T_{12} cages.

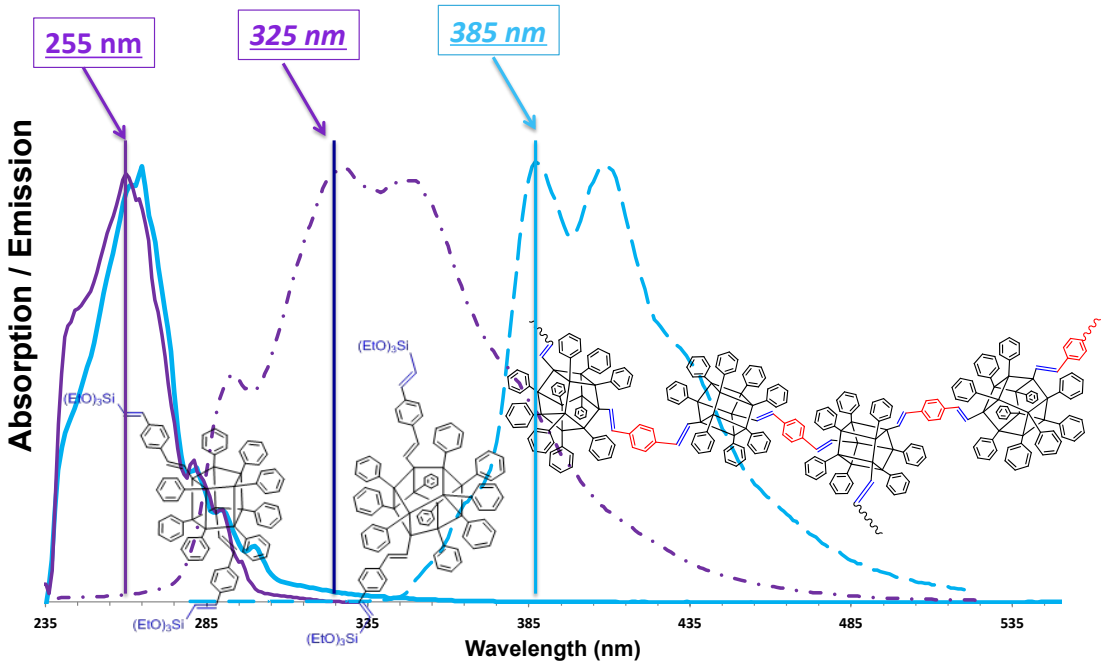

Figure 23. Solution absorption and emission spectra (THF, $\lambda_{excitation}$ = 265 nm) of "beads on a chain" and the corresponding model -Si(OEt)$_3$ compounds [Reproduced from ref. 111 with permission from American Chemical Society, 2010].[111]

These results indicate that unconventional conjugation is not exclusive to T_8 cages but can also be observed in T_{10} and T_{12} cages as might have been expected from the Figure **11** modeling results. With these results in hand, we were able to expand the BoC concept to other cages. One approach was to copolymerize I_8OPS with divinylbenzene followed by functionalization of the remaining iodides, Figure **24**.[114] Unexpectedly the first step gave polymers with DPs ≥20 before further functionalization. Alternately, an average of 6 iodides were first functionalized and then the remaining two iodides copolymerized as shown in Figure **25** for the dialkynyl copolymers.[114]

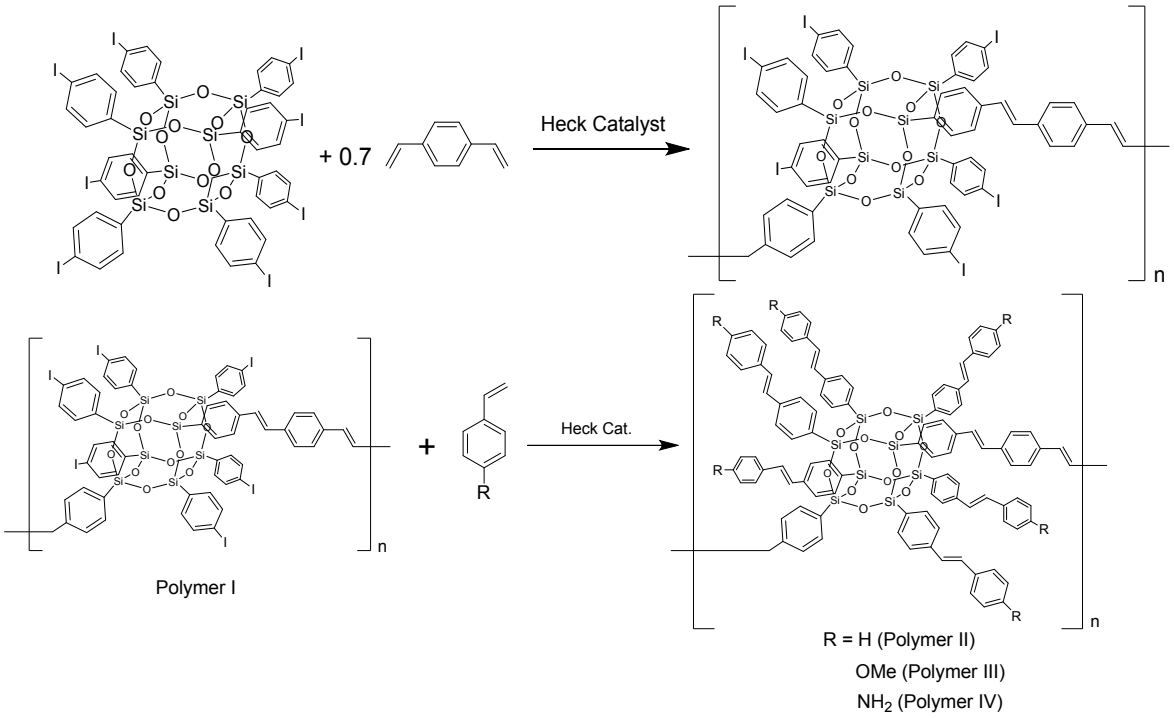

Figure 24. Copolymerization of divinylbenzene with I_8OPS then further functionalization [Reproduced from ref. 114 with permission from American Chemical Society, 2013].[114]

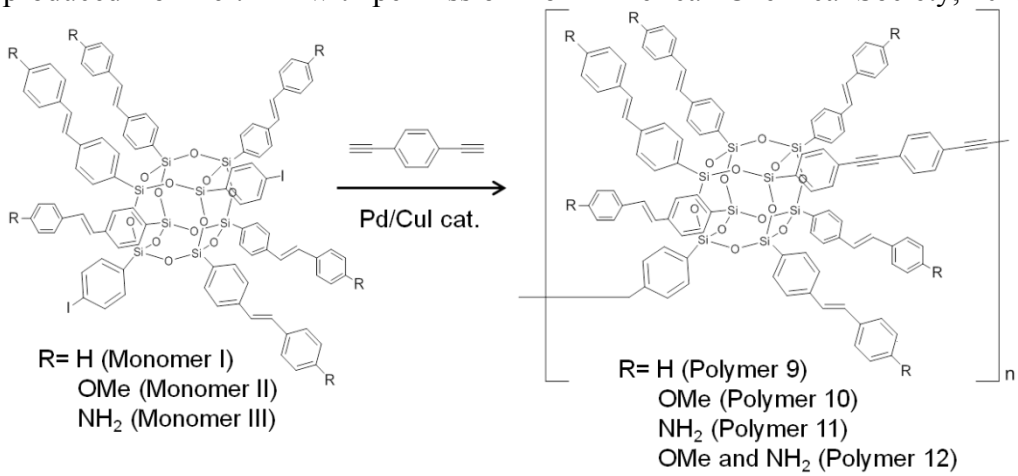

Figure 25. Syntheses of dialkynyl copolymers [Reproduced from ref. 114 with permission from American Chemical Society, 2013].[114]

Perhaps most important to this review comes from copolymerization with two different monomers to generate a terpolymer as presented in Figure **25**. Figure **26** provides absorption/emission spectra for copolymers of diethynylbenzene with monomer II (methoxystilbene) and monomer III (aminostilbene). The diethynylbenzene terpolymer emission is red shifted ≈20 nm compared with the methoxystilbene co-polymer (P 10). This suggests that the energy levels of the copolymer differ from their homopolymers arising from communication of each different SQ cages via conjugation. The terpolymer emission averages those of the two copolymers.

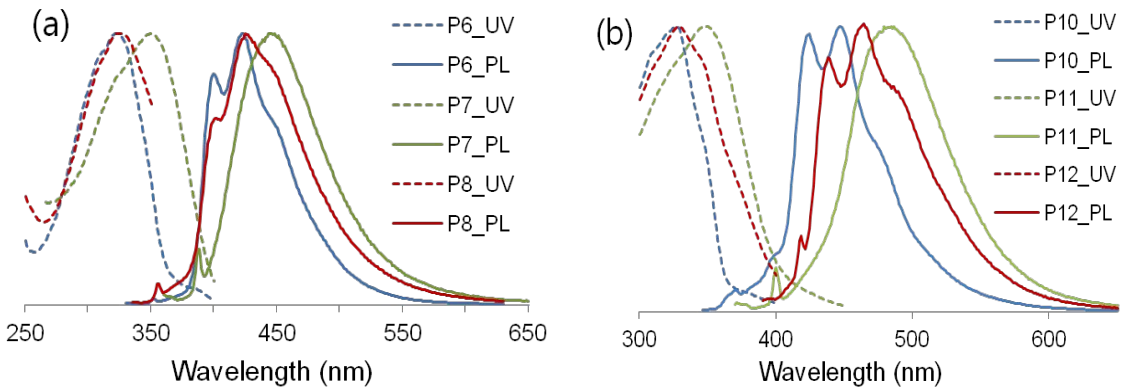

Figure 26. UV-vis and emission spectra for methoxystilbene polymers, aminostilbene polymers and their terpolymers in THF [Reproduced from ref. 113 with permission from American Chemical Society, 2013].[113]

At this point, we sought to expand the generality of unconventional conjugation in SQs exploring the effects of removing a cage corner and opening the cage twice as suggested in Figures **27** and **28** followed by functionalizing via halogenation and subsequent cross coupling.[115]

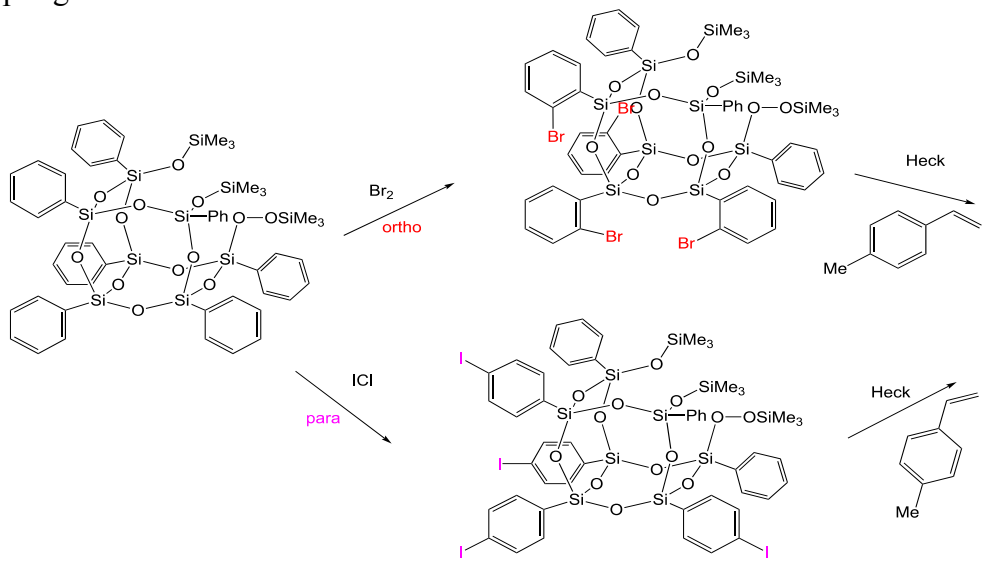

Figure 27. Capping of commercially available trisilanol allows further functionalization.[115]

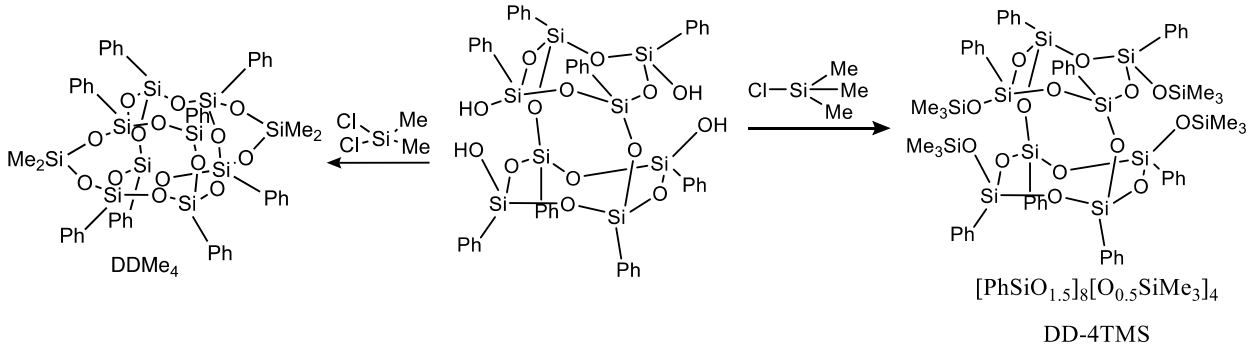

Figure 28. Capping of commercially available tetrasilanol allows further functionalization [Reproduced from ref. 116 with permission from American Chemical Society, 2019].[116]

In both systems, we continue to see red-shifted emissions as witnessed in Figures **29** and **30**.

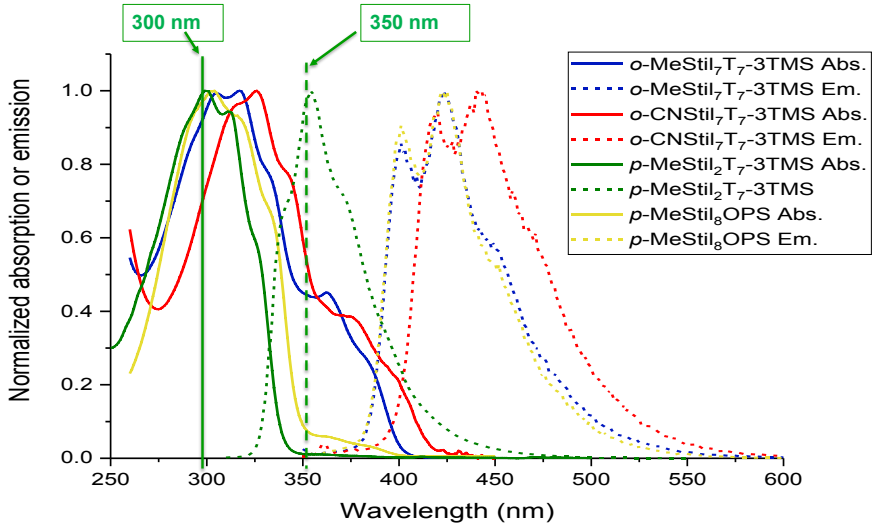

Figure 29. Photophysical characterization of corner missing phenyl cage [Reproduced from ref. 115 with permission from American Chemical Society, 2019].[115]

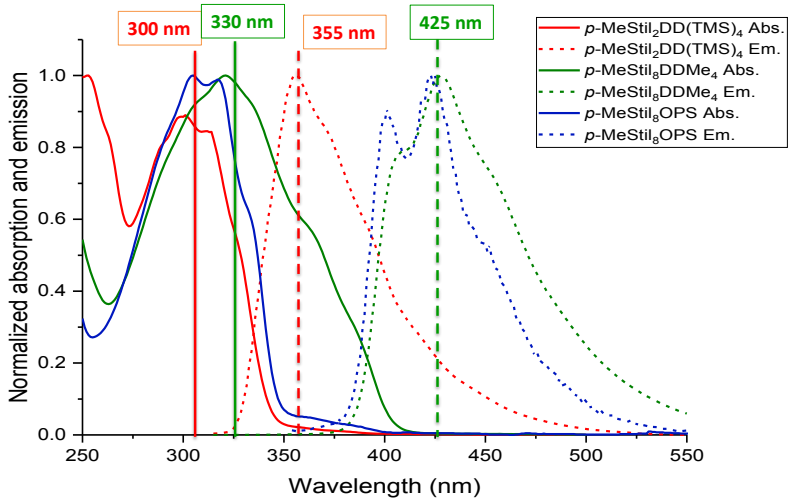

Figure 30. Photophysical characterization of capped tetrasilanol phenyl cage [Reproduced from ref. 116 with permission from American Chemical Society, 2019].[116]

Thus, cage centered LUMOs and 3-D conjugation appear to occur when a corner is missing or two oxygen bridges are broken suggesting a LUMO forms between two face-to-fact silsesquioxane rings. Perhaps most pertinent is the finding in both figures that if only two phenyl groups on average are transformed to stilbenes no red-shift is observed and emission is typical of isolated stilbenes suggesting no conjugation. This implies that LUMO formation onset requires more than two appended conjugated moieties to reduce the energetics for interaction with a LUMO generated within the cage. However, there are several related photophysical effects that should be noted based on data presented in Table **5** below.

However, it is only recently that research has uncovered photophysical behavior that suggests that pendant conjugated groups can interact with SQ cores providing photonic properties that can best be explained by 3-D conjugation through these cores, unconventional conjugation.[117,109,106,118,119] The explanation for this behavior is the formation of Φ_F measured for most stilbene compounds are quite low, typically < 10 % as the excited state is more prone to result in cis-trans isomerization than emission of a photon. Thus, the very much higher Φ_F values seen for the MeStilbene corner missing cage compounds and the doubly open cages is unexpected. Even the doubly substituted corner missing cage which emits in the same place as simple 4-methylstilbene offers a Φ_F= 0.73 vs 0.07. The most reasonable explanation is that the excited state resides primarily in the cage center and is thus protected from solvent promoted radiationless decay. This again points to the cage LUMO playing a role in the photophysical properties of these compounds.

Table 5. Photophysical data for corner missing, doubly open, and tetramethyl capped cages [Reproduced from ref. 115 with permission from American Chemical Society, 2019].[115]

	Abs. λ_{max} (nm)	Em. λ_{max} (nm)	$E_{stoke's}$ (cm^{-1})	Φ_F(-)	TPA-δ (GM)
p-MeStilbene	298, 311	355		**0.07**	
vinylDDvinyl	265	312, 330			
p-MeStil$_8$OPS	305, 320	400, 422	9090	0.57	1.4
o-MeStil$_7$T$_7$(OTMS)$_3$	304, 317	406, 418	7790	**0.81**	0.7
o-MeStil$_2$Ph$_5$T$_7$(OTMS)$_3$	299, 311	354	5196	**0.73**	--
o-MeStil$_7$DDMe$_4$	305, 316	403, 426	8170	0.69	2.9
o-CNStil$_7$DDMe$_4$	317, 325	420, 442	8145	0.36	17
p-MeStil$_8$DDMe$_4$	321	427	7730	0.28	6.3
o-Br$_7$DD(OTMS)$_4$	272	312			
o-MeStil$_7$DD(OTMS)$_4$	305, 317	401, 421	7793	**0.75**	2.5
o-CNStil$_7$DD(OTMS)$_4$	314, 326	420, 442	8050	0.48	37
p-MeStil$_2$DD(OTMS)$_4$	305	355	5054	0.10	2.7
p-MeStil$_7$DD(OTMS)$_4$	330	408, 425			

In this set of studies, we were also able to use an unusual spectroscopic method of characterization that explores molecular responses to intense laser light that generates high frequency magnetic fields that can be correlated with molecular structure.[115] The method relies on non-linear magnetoelectric scattering characterization from excitation with intense laser light. Details of the methods and characterization techniques can be found here and references therein.[115] The results of these studies find further evidence for formation of spherical excited state LUMOs adding further corroboration for unconventional conjugation.

The next step in expanding the number of SQs that offer unconventional conjugation was to examine the functionalization of the vinyl groups in the divinyl double decker (vinyl$_2$DD) system as suggested by Figure **31**.[120,121] Our original expectation was that the double caping with disiloxane linkages should lead to the end to possible conjugation. Thus, finding we were incorrect was perhaps one of the more surprising discoveries as illustrated in Figure **32**.

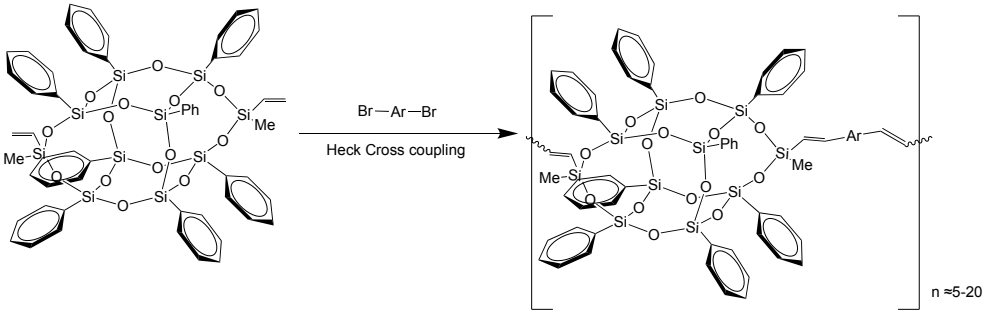

Figure 31. Copolymerization of vinyl$_2$DD with dibromoaromatic compounds[Reproduced from ref. 116 with permission from American Chemical Society, 2019].[116]

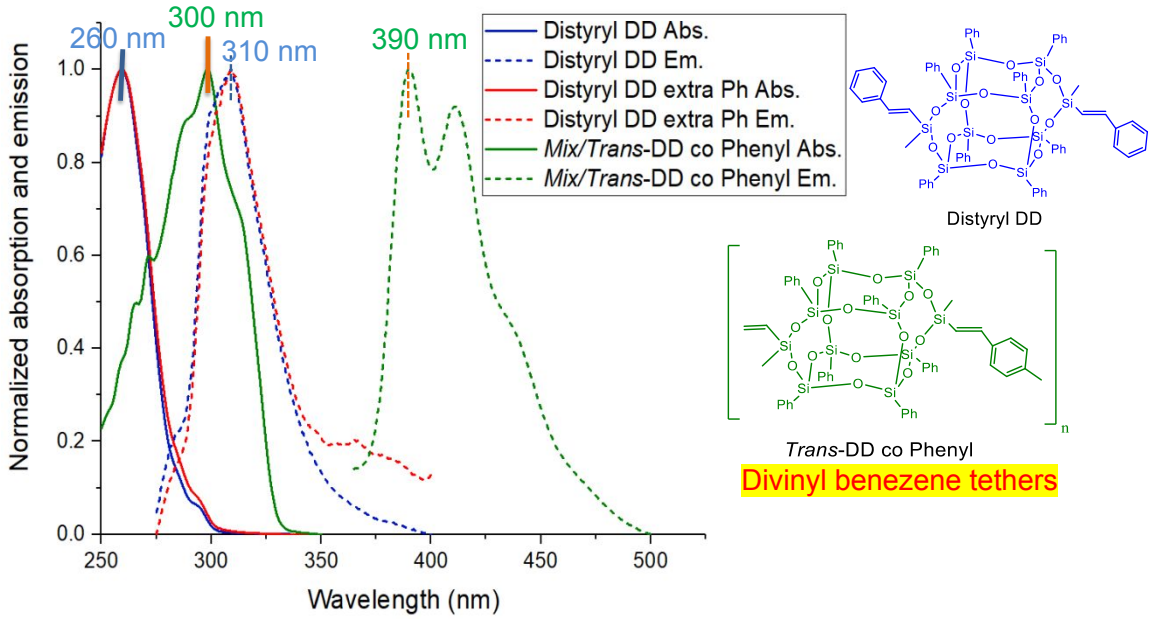

Figure 32. Photophysics of [vinylDDvinyl-Ph]$_x$ where x >20.

The model distyrenyl compound behaves as expected with an absorption λ_{max} = 260 nm and an emission λ_{max} = 310 nm. Although the vinylbenzene copolymer offers an absorption λ_{max} = 300 nm, the observed emission λ_{max} = 390 nm matches that of the divinylbenzene copolymer of Figure **23** suggesting conjugation despite the two disiloxane caps in each DD monomer unit.

Figure **33** provides another example but for a copolymer with thiophene revealing a further red-shift. In general, introducing thiophene based co-monomers gives red-shifts > 100 nm with respect to copolymers with phenyl, biphenyl and terphenyl. Table **6** provides data from a recent publication.[121] Note that the thiophene copolymers all offer Φ_F values that are much lower than the all carbon aromatic co-monomers suggesting alternate radiationless decay process(es) not available to these systems.

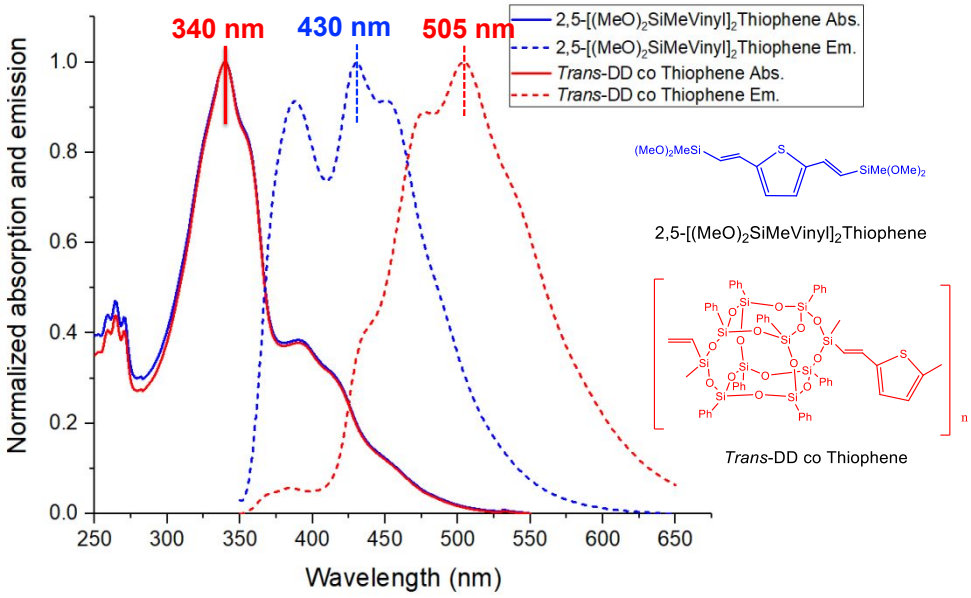

Figure 33. Photophysics of [vinylDDvinyl-thiophene]$_x$ where x >20.

Table 6. GPC and steady-state photophysical data for vinylDDvinyl co-polymers [Reproduced from ref. 120 with permission from American Chemical Society, 2020].[120]

	GPC			Abs. λ_{max} (nm)	Em. λ_{max} (nm)	Φ_F
	M_n	M_w	Đ			
Vinyl(Me)DD(Me)vinyl	1010	1080	1.07	264	281	
DD-co-phenyl	19550	49410	2.53	298	390, 412	0.08±0.001
DD-co-biphenyl	11690	24480	2.09	314	357, 373	0.66±0.05
DD-co-terphenyl	15780	34770	2.20	321	374, 392	0.87±0.04
DD-co-stilbene	9210	25390	2.76	357	393, 412, 436	0.61±0.04
DD-co-thiophene	22540	43250	1.92	340	478, 505	0.09±0.001
DD-co-bithiophene	3580	7200	2.01	391	505, 538	0.17±0.02
DD-co-thienothiophene	4480	10040	2.24	358	496, 526	0.13±0.01
DD-co-9,9-dimethylfluorene	20790	46100	2.22	339, 353	424, 448	0.34±0.003
DD-co-benzothiadiazole	8390	17380	2.07	392	481	0.22±0.003
DD-co-carbazole	13680	33850	2.47	301	373, 392	0.41±0.02

One further proof of conjugation in these systems comes from studies of their interactions with F_4TCNQ where the conjugated polymer can donate an electron to F_4TCNQ generating a radical anion.

Thus, selected DD copolymers and model cage compounds were mixed with F_4TCNQ via the mixed-solution method.[122,123] A yellow-orange CH_2Cl_2 solution of F_4TCNQ was added to bright orange to red colored solutions of DD-co-thiophene, -bithiophene and -thienothiophene. The resulting solutions turn *dark green to black*, depending on the mole percent F_4TCNQ added. One can also observe electron transfer via shifts in νC≡N associated with charge transfer (CT) promoted color-changes, Figure **34**.

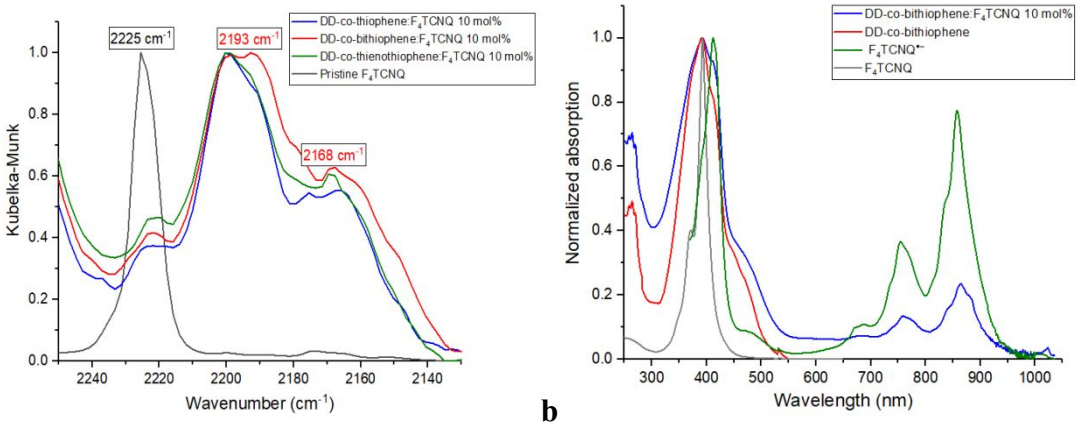

Figure 34. (a) The characteristic region of νC≡N in FTIR spectra for DD-co-thiophene, -bithiophene, -thienothiophene mixing with 10 mol% F_4TCNQ and pristine F_4TCNQ [Reproduced from ref. 121 with permission from Wiley, 2021].[121]

Given that it appears disiloxane capped doubled decker (DD) copolymers exhibit conjugation, we have very recently synthesized terpolymers of these systems akin to the results reported in Figure **26**.[114] Our approach is presented in Figure **35**. Examples of both co- and ter-polymer photophysical characterization data are presented in Figure **36**, related data available elsewhere.[124]

The most important observation is that as with the earlier work, the terpolymer emission $\lambda_{max} \approx 490$ nm is the average of the two co-monomers meaning that the terpolymer shows conjugation through the backbone and delocalization must occur that involves all components supporting our continuing efforts to expand our understanding of conjugation in these systems.

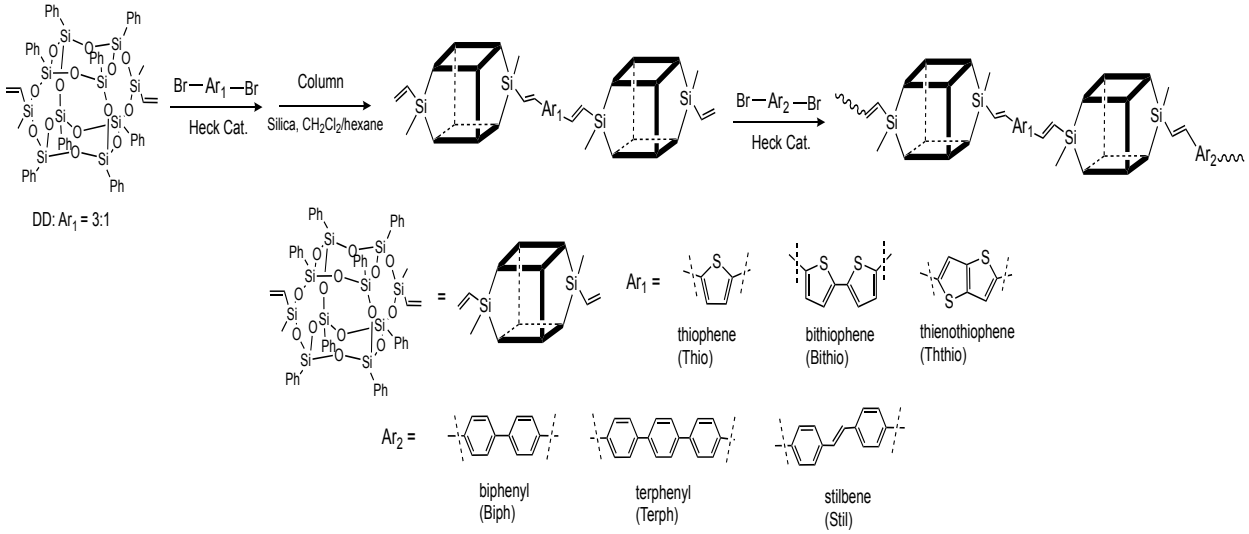

Figure 35. General approach to synthesizing DD based alternating terpolymers.[124]

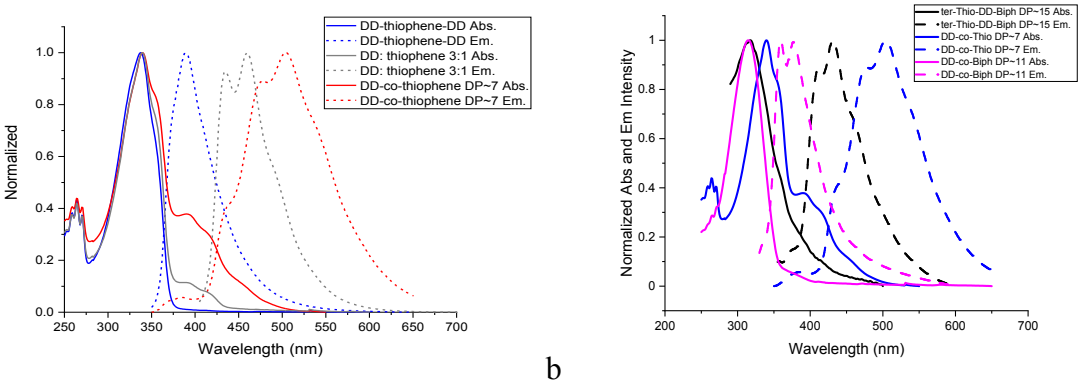

a b

Figure 36a. Normalized absorption and emission of DD-thiophene-DD, mixture of DD:thiophene 3:1 and longer DD-co-thiophene (1:1). **b**. Absorption and emission of ter-thio-DD-biph and corresponding copolymers, DD-co-biphenyl and DD-co-thiophene.[124]

At this point, we were able to explore still another type of silsesquioxane system synthesized by the Unno group in Gunma University; ladder compounds which do not have cages but do have vinyldisiloxane caps (vinyl$_2$LL), Figure **37**.[125] Given the above premise that a cage format or at least opposing silsesquioxane rings (doubly open, Figure **28**) is required for a LUMO to form, it seemed reasonable that the lack of a cage would preclude formation of an internal LUMO. Thus, we synthesized LL analogs of the DD copolymers (see Figure **31**).

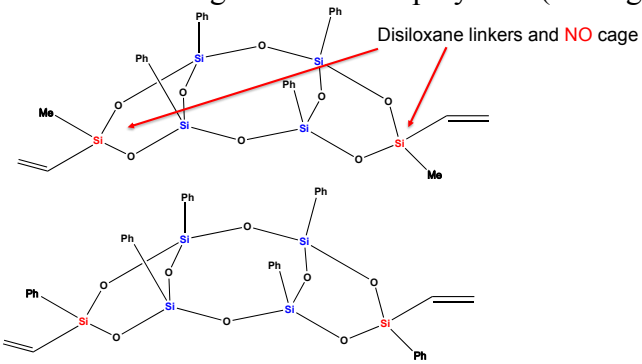

Figure 37. vinyldisiloxane capped ladder (LL) silsesquioxane [Reproduced from ref. 125 with permission from American Chemical Society, 2019].[125]

Figure **38** compares the photophysical properties of the DD-phenyl model, DD-co-phenyl (DP 12) with the LL-co-phenyl (DP 4) unexpectedly revealing further red-shifts in λ_{max} to 415 nm from 390 nm.[121] These results mean that a cage centered LUMO may not be the only mechanism whereby conjugation occurs. As with the DD copolymers, the longer the chain the further the red shift as seen for LL-co-thiophene in Figure **39**. All of the λ_{max} are shifted further red than with the DD copolymers indicating better conjugation---without a cage!

Table **7** records the properties of the various LL-co-polymers synthesized to date.[121] As with the DD copolymers, we also find that the LL copolymers interact with F_4TCNQ, Figure **40**.

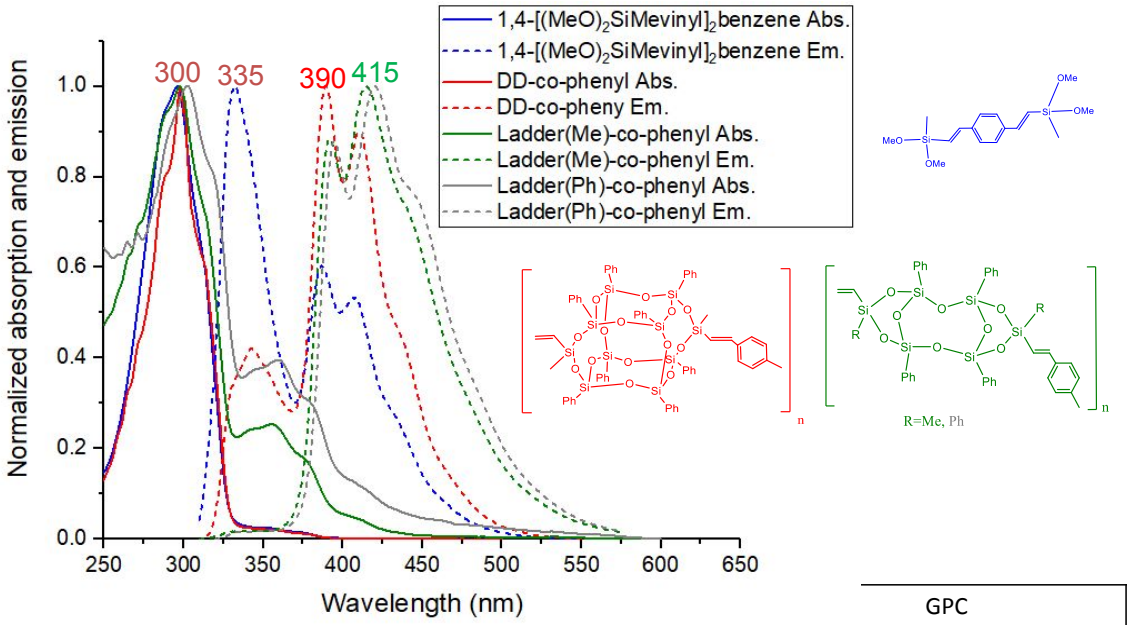

	GPC			
	M_n	M_w	PDI	DP
DD-co-phenyl	14500	39200	2.71	~12
Ladder(Me)-co-phenyl	3700	7600	2.05	~4
Ladder(Ph)-co-phenyl	3500	7100	2.01	~4

Figure 38. Uv/vis spectra of DD-co-phenyl, LL-co-phenyl and model compound [Reproduced from ref. 121 with permission from Wiley, 2021].[121]

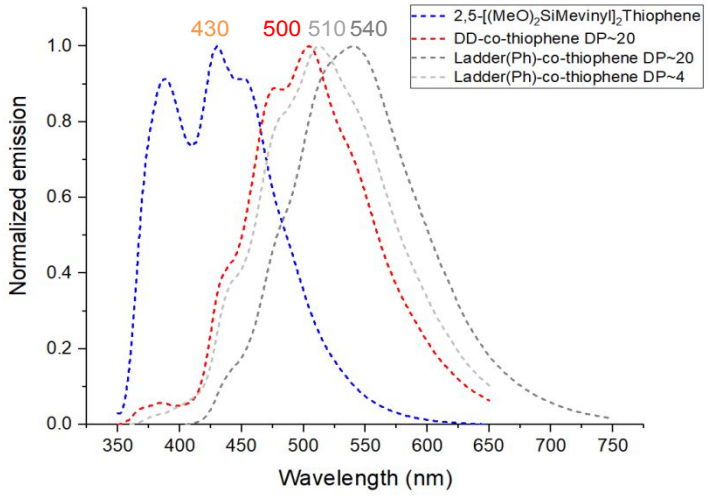

Figure 39. Uv/vis spectra of DD-co-thiophene, LL-co-thiophene vs DP and model compound [Reproduced from ref. 121 with permission from Wiley, 2021].[121]

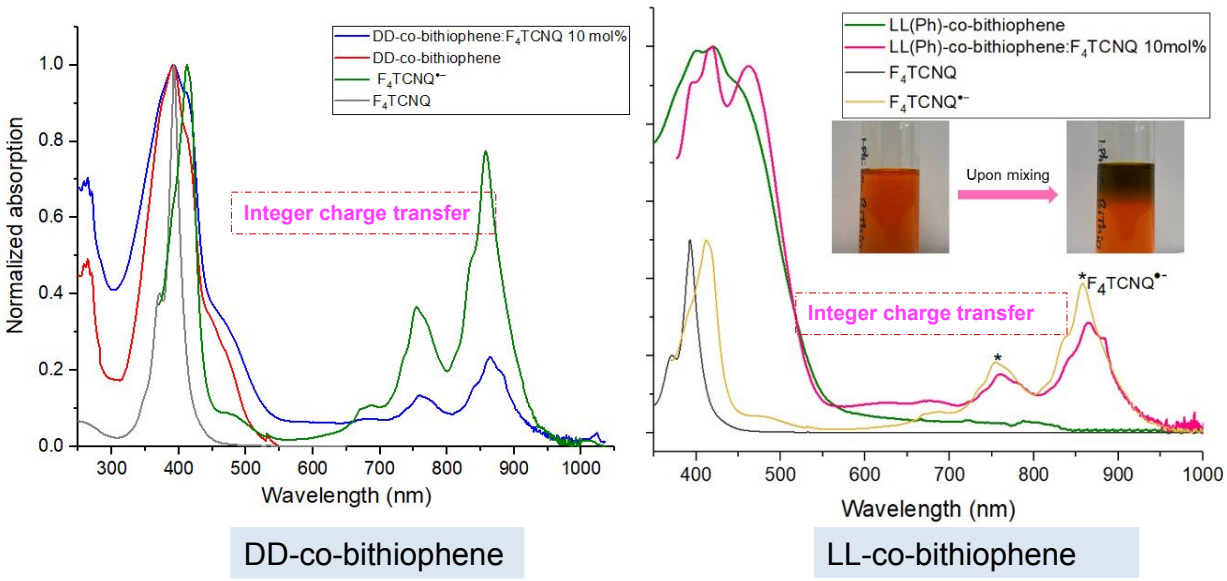

Figure 40. Solution mixing of F_4TCNQ CT with DD-co-bithiophene and LL-co-bithiophene revealing integer charge transfer [Reproduced from ref. 121 with permission from Wiley, 2021].[121]

Table 7. GPC and steady-state photophysical data for vinyl$_2$LL co-polymers [Reproduced from ref. 126 with permission from the American Chemical Society, 2020].[126]

	GPC			Abs. λ_{max} (nm)	Em. λ_{max} (nm)	Φ_F
	M_n	M_w	Đ			
Vinyl-LL(Me)-vinyl	490	530	1.08	264	281	
Vinyl-LL(Ph)-vinyl	540	620	1.15	265	285	
LL1: LL-co-phenyl	5420	15190	2.80	298	392, 415	
LL2: LL-co-biphenyl	4810	11730	2.44	312	412, 430	0.45718
LL3: LL-co-terphenyl	15850	46580	2.95	321	378, 418, 437	0.61±0.02
LL4: LL-co-stilbene	6280	19620	3.12	356	448, 472	0.35±0.03
LL5: LL-co-thiophene	5600	16070	2.87	343	540	
LL6: LL-co-bithiophene	5540	11330	2.05	392	550	0.07307
LL7: LL-co-thienothiophene	5290	10470	1.98	356, 371	530	0.09346
LL8: LL-co-dimethylfluorene	5810	15780	2.72	337, 353	383, 426, 451	0.68±0.02
LL9: LL-co-benzothiadiazole	2750	5130	1.87	285, 393	493	0.04285
LL10: LL-co-carbazole	2580	4300	1.67	259, 298	403	0.24451

We are currently in the process of synthesizing LL terpolymer systems; unfortunately, this system is quite fragile and subject to ring opening polymerization if not carefully worked up.

Now we have a conundrum; how does conjugation occur and how can it be modeled? To date, we have worked with two groups that have attempted to model conjugation in these systems using DFT modeling methods VASP and Gaussian 16.[124] Unfortunately, both approaches cannot identify LUMOs delocalized across DD-co-monomer units. These results are not surprising because of the unconventional behavior of these systems.

Indeed, preliminary TPA studies of the DD- and LL- copolymer systems, find that they deviate from Kasha's rule in that many of these compounds exhibit different emissions depending on the excitation wavelength used.

For example: “the fluorescence emission spectra of many if not all studied so far SQ-based systems defy Kasha’s rule, i.e. there appears to be a notable shift of the emission spectrum depending on the excitation wavelength. As an immediate consequence, measurements of 2PA cross-sections and 2PA spectra that rely on detection of fluorescence; in particular, such as reported recently[126] may yield largely varying values, depending on what part of the fluorescence signal is being detected.

Indeed, “the maximum 2PA cross sections in the series vary greatly, depending on the Ar substituent, *by more than one order of magnitude*. In some cases, these variations correlate and in some cases do not with the behavior observed in the 2PEF (photon emission fluorescence) measurements performed on the exact same systems. For example, the highest non-linear transmittance-based 2PA cross sections are obtained with benzothiadiazole, σ_{2PA} (780 – 550 nm) = 100 - 600 GM, and carbazole, σ_{2PA} (700 – 550 nm) = 100 - 400 GM.”[127]

For both DD-copolymers, these values are more than an order of magnitude larger than reported previously using the 2PEF method, which may be related to deviation from Kasha’s rule or caused by a very strong ESA effect or both. An expansion of these results will be published at a later date.[127]

Conclusions

It is extremely rare to find new forms of conjugation especially in molecular structures where one expects insulating behavior (e.g. with disiloxane bridging caps) given the traditional view of these components. We attempt here to review a number of systems where conjugation is not simply via π-π overlap or related, known forms of conjugation. The latter are found when non-carbon elements are included in the main chain that provide empty *p* orbitals, which is especially true for boron containing systems. When the non-carbon elements can form double bonds, then traditional π-π overlap again is the primary mechanism for delocalization/conjugation.

Our overall observation is that unconventional conjugation seems to occur in 3-D structures including carboranes, metal clusters, and in particular silsesquioxanes. In each case, the mechanisms of conjugation where understood can involve electron delocalization including via intervalence charge transfer within the clusters or via radical anion electron transfer. To date, the mechanism(s) whereby conjugation occurs in silsesquioxanes; given the above multiple examples, remains unknown despite multiple efforts to model the photophysical behavior of these systems.

Given the considerable published (patented) efforts to modify the properties of well-known conjugated polymer systems with the many resulting commercial applications; one might suggest that further efforts to expand our knowledge of the various manipulable properties of these newly discovered silsesquioxane systems might also lead to commercially important materials.

Clearly, there is an opportunity to develop new modeling methods but the method of approach at present remains to be defined. Given the successful modeling to date (Figure **11**),[102] and the magnetic field generation results,[115] we would have been very happy to suggest that formation of cage centered LUMOs as the simplest explanation. However, recent results with ladder polymers that exhibit even further red-shifts than the cage SQs studied previously but have no cage, likely suggest one or more unique delocalization processes.

The identification of multiple systems that exhibit conjugation but not via traditional mechanisms perhaps requires a broader definition of conjugation: One that involves charge delocalization across multiple components or moieties both organic and inorganic that substantially lowers system energies/band gaps. As with the traditional polymers noted at the

outset, the potential for new semi-, conducting and perhaps superconducting behavior represent challenges to both model and expand our knowledge base vis a vis silsesquioxane macromonomer and polymer systems.

Finally, this story is not finished as we have now begun to study the photophysical properties of the following more extreme examples of silsesquioxanes:

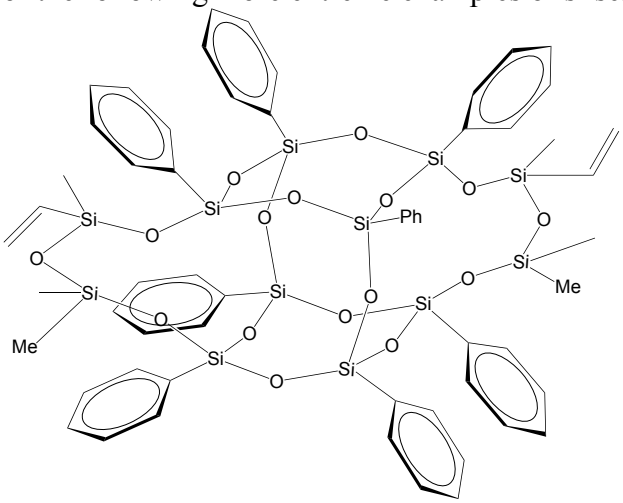

tetra(vinylmethyldisiloxane) capped DD, $Vinyl_4XDD$

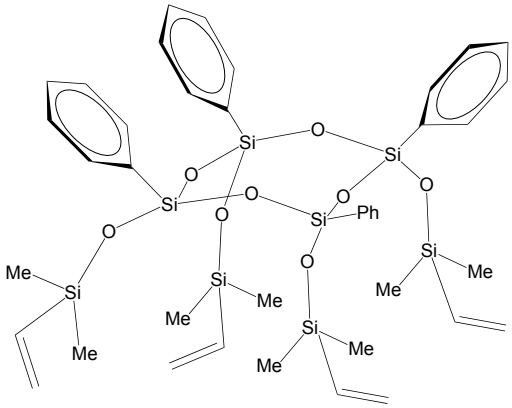

tetra(vinyldimethylsiloxane) capped half cage

Copolymers of both systems also show what appears to be extended conjugation which will be the subject for a future publication.

Acknowledgements

We would like to thank NSF for the funding that supports this work through Chem. Awards 1610344 and 2103602. Zijing Zhang is thanked for finding some of the references used in the introduction section.

References

(1) Reynolds, J. R.; Thompson, B. C.; Skotheim, T. A. *Conjugated Polymers: Perspective, Theory, and New Materials*; 2019.

(2) Rasmussen, S. C. Conjugated and Conducting Organic Polymers: The First 150 Years. *ChemPlusChem* **2020**, *85* (7), 1412–1429. https://doi.org/10.1002/cplu.202000325.

(3) Bradley, D. D. C. Conjugated Polymer Electroluminescence. *Synthetic Metals* **1993**, *54* (1–3), 401–415. https://doi.org/10.1016/0379-6779(93)91086-H.

(4) Birgerson, J.; Fahlman, M.; Bröms, P.; Salaneck, W. R. Conjugated Polymer Surfaces and Interfaces: A Mini-Review and Some New Results. *Synthetic Metals* **1996**, *80* (2), 125–130. https://doi.org/10.1016/S0379-6779(96)03692-2.

(5) Tessler, N.; Denton, G. J.; Friend, R. H. Lasing from Conjugated-Polymer Microcavities. *Nature* **1996**, *382* (6593), 695–697. https://doi.org/10.1038/382695a0.

(6) Günes, S.; Neugebauer, H.; Sariciftci, N. S. Conjugated Polymer-Based Organic Solar Cells. *Chem. Rev.* **2007**, *107* (4), 1324–1338. https://doi.org/10.1021/cr050149z.

(7) Coakley, K. M.; McGehee, M. D. Conjugated Polymer Photovoltaic Cells. *Chem. Mater.* **2004**, *16* (23), 4533–4542. https://doi.org/10.1021/cm049654n.

(8) Neo, W. T.; Ye, Q.; Chua, S.-J.; Xu, J. Conjugated Polymer-Based Electrochromics: Materials, Device Fabrication and Application Prospects. *J. Mater. Chem. C* **2016**, *4* (31), 7364–7376. https://doi.org/10.1039/C6TC01150K.

(9) Palani, P.; Karpagam, S. Conjugated Polymers – a Versatile Platform for Various Photophysical, Electrochemical and Biomedical Applications: A Comprehensive Review. *New J. Chem.* **2021**, *45* (41), 19182–19209. https://doi.org/10.1039/D1NJ04062F.

(10) McQuade, D. T.; Pullen, A. E.; Swager, T. M. Conjugated Polymer-Based Chemical Sensors. *Chem. Rev.* **2000**, *100* (7), 2537–2574. https://doi.org/10.1021/cr9801014.

(11) Mike, J. F.; Lutkenhaus, J. L. Recent Advances in Conjugated Polymer Energy Storage. *J. Polym. Sci. B Polym. Phys.* **2013**, *51* (7), 468–480. https://doi.org/10.1002/polb.23256.

(12) Tuncel, D.; Demir, H. V. Conjugated Polymer Nanoparticles. *Nanoscale* **2010**, *2* (4), 484. https://doi.org/10.1039/b9nr00374f.

(13) Morin, P.-O.; Bura, T.; Leclerc, M. Realizing the Full Potential of Conjugated Polymers: Innovation in Polymer Synthesis. *Mater. Horiz.* **2016**, *3* (1), 11–20. https://doi.org/10.1039/C5MH00164A.

(14) Sanzone, A.; Calascibetta, A.; Monti, M.; Mattiello, S.; Sassi, M.; Corsini, F.; Griffini, G.; Sommer, M.; Beverina, L. Synthesis of Conjugated Polymers by Sustainable Suzuki Polycondensation in Water and under Aerobic Conditions. *ACS Macro Lett.* **2020**, *9* (8), 1167–1171. https://doi.org/10.1021/acsmacrolett.0c00495.

(15) Beaumont, C.; Naqvi, S.; Leclerc, M. Strategies for the Synthesis of Water-Soluble Conjugated Polymers. *Trends in Chemistry* **2022**, S2589597422001253. https://doi.org/10.1016/j.trechm.2022.05.002.

(16) Etemad, S.; Heeger, A. J. Polyacetylene, (CH)x: The Prototype Conducting Polymer. *Annu. Rev. Phys. Chem.* **1982**, *33* (1), 443–469. https://doi.org/10.1146/annurev.pc.33.100182.002303.

(17) Chien, J. C. W. *Polyacetylene: Chemistry, Physics, and Material Science*; Academic Press: New York, 1984.

(18) Lopyrev, V. A.; Myachina, G. F.; Shevaleyevskii, O. I.; Khidekel, M. L. Polyacetylene. Review. *Polymer Science U.S.S.R.* **1988**, *30* (10), 2151–2173. https://doi.org/10.1016/0032-3950(88)90348-6.

(19) Masuda, T. Substituted Polyacetylenes. *J. Polym. Sci. A Polym. Chem.* **2007**, *45* (2), 165–180. https://doi.org/10.1002/pola.21782.
(20) Geniès, E. M.; Boyle, A.; Lapkowski, M.; Tsintavis, C. Polyaniline: A Historical Survey. *Synthetic Metals* **1990**, *36* (2), 139–182. https://doi.org/10.1016/0379-6779(90)90050-U.
(21) Bhadra, S.; Khastgir, D.; Singha, N. K.; Lee, J. H. Progress in Preparation, Processing and Applications of Polyaniline. *Progress in Polymer Science* **2009**, *34* (8), 783–810. https://doi.org/10.1016/j.progpolymsci.2009.04.003.
(22) Zare, E. N.; Makvandi, P.; Ashtari, B.; Rossi, F.; Motahari, A.; Perale, G. Progress in Conductive Polyaniline-Based Nanocomposites for Biomedical Applications: A Review. *J. Med. Chem.* **2020**, *63* (1), 1–22. https://doi.org/10.1021/acs.jmedchem.9b00803.
(23) Beygisangchin, M.; Abdul Rashid, S.; Shafie, S.; Sadrolhosseini, A. R.; Lim, H. N. Preparations, Properties, and Applications of Polyaniline and Polyaniline Thin Films—A Review. *Polymers* **2021**, *13* (12), 2003. https://doi.org/10.3390/polym13122003.
(24) McCullough, R. D. The Chemistry of Conducting Polythiophenes. *Adv. Mater.* **1998**, *10* (2), 93–116. https://doi.org/10.1002/(SICI)1521-4095(199801)10:2<93::AID-ADMA93>3.0.CO;2-F.
(25) Perepichka, I. F.; Perepichka, D. F.; Meng, H.; Wudl, F. Light-Emitting Polythiophenes. *Adv. Mater.* **2005**, *17* (19), 2281–2305. https://doi.org/10.1002/adma.200500461.
(26) Mehmood, U.; Al-Ahmed, A.; Hussein, I. A. Review on Recent Advances in Polythiophene Based Photovoltaic Devices. *Renewable and Sustainable Energy Reviews* **2016**, *57*, 550–561. https://doi.org/10.1016/j.rser.2015.12.177.
(27) Kaloni, T. P.; Giesbrecht, P. K.; Schreckenbach, G.; Freund, M. S. Polythiophene: From Fundamental Perspectives to Applications. *Chem. Mater.* **2017**, *29* (24), 10248–10283. https://doi.org/10.1021/acs.chemmater.7b03035.
(28) Ateh, D. D.; Navsaria, H. A.; Vadgama, P. Polypyrrole-Based Conducting Polymers and Interactions with Biological Tissues. *J. R. Soc. Interface.* **2006**, *3* (11), 741–752. https://doi.org/10.1098/rsif.2006.0141.
(29) Omastová, M.; Mičušík, M. Polypyrrole Coating of Inorganic and Organic Materials by Chemical Oxidative Polymerisation. *Chemical Papers* **2012**, *66* (5). https://doi.org/10.2478/s11696-011-0120-4.
(30) Jain, R.; Jadon, N.; Pawaiya, A. Polypyrrole Based next Generation Electrochemical Sensors and Biosensors: A Review. *TrAC Trends in Analytical Chemistry* **2017**, *97*, 363–373. https://doi.org/10.1016/j.trac.2017.10.009.
(31) Pang, A. L.; Arsad, A.; Ahmadipour, M. Synthesis and Factor Affecting on the Conductivity of Polypyrrole: A Short Review. *Polym Adv Technol* **2021**, *32* (4), 1428–1454. https://doi.org/10.1002/pat.5201.
(32) Smith, R. C.; Protasiewicz, J. D. Conjugated Polymers Featuring Heavier Main Group Element Multiple Bonds: A Diphosphene-PPV. *J. Am. Chem. Soc.* **2004**, *126* (8), 2268–2269. https://doi.org/10.1021/ja0394683.
(33) Wright, V. A.; Patrick, B. O.; Schneider, C.; Gates, D. P. Phosphorus Copies of PPV: π-Conjugated Polymers and Molecules Composed of Alternating Phenylene and Phosphaalkene Moieties. *J. Am. Chem. Soc.* **2006**, *128* (27), 8836–8844. https://doi.org/10.1021/ja060816l.
(34) Suematsu, K.; Nakamura, K.; Takeda, J. Polyimine, a C=N Double Bond Containing Polymers: Synthesis and Properties. *Polym J* **1983**, *15* (1), 71–79. https://doi.org/10.1295/polymj.15.71.

(35) Manabe, Y.; Uesaka, M.; Yoneda, T.; Inokuma, Y. Two-Step Transformation of Aliphatic Polyketones into π-Conjugated Polyimines. *J. Org. Chem.* **2019**, *84* (16), 9957–9964. https://doi.org/10.1021/acs.joc.9b01119.
(36) Sibaprasad Bhattacharyya; Sangita Zaleski; Jeffrey M. Zaleski. Unique Meta-Diyne,-ENyne and -Endiyne Complexes: Part If the Remarkably Diverse World of Metal-Alkyne Chemistry; Progress in Inorganic Chemistry; Vol. 55, pp 355–482.
(37) Wong, W.-Y. Transition Metal σ-Acetylide Polymers Containing Main Group Elements in the Main Chain: Synthesis, Light Emission and Optoelectronic Applications. In *Inorganic and Organometallic Macromolecules*; Abd-El-Aziz, A. S., Carraher, C. E., Pittman, C. U., Zeldin, M., Eds.; Springer New York: New York, NY, 2008; pp 37–69. https://doi.org/10.1007/978-0-387-72947-3_3.
(38) Mei, J.; Ogawa, K.; Kim, Y.-G.; Heston, N. C.; Arenas, D. J.; Nasrollahi, Z.; McCarley, T. D.; Tanner, D. B.; Reynolds, J. R.; Schanze, K. S. Low-Band-Gap Platinum Acetylide Polymers as Active Materials for Organic Solar Cells. *ACS Appl. Mater. Interfaces* **2009**, *1* (1), 150–161. https://doi.org/10.1021/am800104k.
(39) Dubinina, G. G.; Price, R. S.; Abboud, K. A.; Wicks, G.; Wnuk, P.; Stepanenko, Y.; Drobizhev, M.; Rebane, A.; Schanze, K. S. Phenylene Vinylene Platinum(II) Acetylides with Prodigious Two-Photon Absorption. *J. Am. Chem. Soc.* **2012**, *134* (47), 19346–19349. https://doi.org/10.1021/ja309393c.
(40) Geserich, H.-P.; Pintschovius, L. Polymeric sulfur nitride, (SN)x—A new type of a one-dimensional metal? In *Festkörperprobleme 16*; Treusch, J., Ed.; Advances in Solid State Physics; Springer Berlin Heidelberg: Berlin, Heidelberg, 1976; Vol. 16, pp 65–94. https://doi.org/10.1007/BFb0107739.
(41) A. G. Macdiarmid; C. M. Mikulski; M. S. Saran; P.J. Russo; M.J. Cohen; A.A. Bright; A. F. Garito; A. J. Heeger. Synthesis and Selected Properties of Polymeric Sulfur Nitride, (Polythiazyl), (SN)x. In *Inorganic Compounds with unusual propertie*; Advances in chemistry series; AMERICAN CHEMICAL SOCIETY, 1976; Vol. 150.
(42) Labes, M. M.; Love, P.; Nichols, L. F. Polysulfur Nitride - a Metallic, Superconducting Polymer. *Chem. Rev.* **1979**, *79* (1), 1–15. https://doi.org/10.1021/cr60317a002.
(43) 4. Sulfur-Based Inorganic Polymers: Polythiazyl and Polythiol. In *Inorganic and Organometallic Polymers*; De Gruyter, 2019; pp 77–87. https://doi.org/10.1515/9781501514609-005.
(44) Aquino, A. J. A.; Soares, L. A.; Da Silva, A. B. F.; Trsic, M. Molecular Orbital Description of the Polythiazyl Polymer. *Journal of Molecular Structure: THEOCHEM* **1986**, *139* (3–4), 327–332. https://doi.org/10.1016/0166-1280(86)87049-X.
(45) Steven D. Gammon. Poly(Sulfur Nitride), (SN)x, Synthesis, Structure, and Conductivity, 1986.
(46) Saito, R.; Hofmann, M.; Dresselhaus, G.; Jorio, A.; Dresselhaus, M. S. Raman Spectroscopy of Graphene and Carbon Nanotubes. *Advances in Physics* **2011**, *60* (3), 413–550. https://doi.org/10.1080/00018732.2011.582251.
(47) Drummer, M. C.; Singh, V.; Gupta, N.; Gesiorski, J. L.; Weerasooriya, R. B.; Glusac, K. D. Photophysics of Nanographenes: From Polycyclic Aromatic Hydrocarbons to Graphene Nanoribbons. *Photosynth Res* **2022**, *151* (2), 163–184. https://doi.org/10.1007/s11120-021-00838-y.

(48) Stergiou, A.; Pagona, G.; Tagmatarchis, N. Donor–Acceptor Graphene-Based Hybrid Materials Facilitating Photo-Induced Electron-Transfer Reactions. *Beilstein J. Nanotechnol.* **2014**, *5*, 1580–1589. https://doi.org/10.3762/bjnano.5.170.
(49) Baker, S. N.; Baker, G. A. Luminescent Carbon Nanodots: Emergent Nanolights. *Angewandte Chemie International Edition* **2010**, *49* (38), 6726–6744. https://doi.org/10.1002/anie.200906623.
(50) Li, H.; Kang, Z.; Liu, Y.; Lee, S.-T. Carbon Nanodots: Synthesis, Properties and Applications. *J. Mater. Chem.* **2012**, *22* (46), 24230. https://doi.org/10.1039/c2jm34690g.
(51) Sciortino, A.; Cannizzo, A.; Messina, F. Carbon Nanodots: A Review—From the Current Understanding of the Fundamental Photophysics to the Full Control of the Optical Response. *C* **2018**, *4* (4), 67. https://doi.org/10.3390/c4040067.
(52) Liu, H.; Ye, T.; Mao, C. Fluorescent Carbon Nanoparticles Derived from Candle Soot. *Angew. Chem. Int. Ed.* **2007**, *46* (34), 6473–6475. https://doi.org/10.1002/anie.200701271.
(53) Wang, X.; Qu, K.; Xu, B.; Ren, J.; Qu, X. Multicolor Luminescent Carbon Nanoparticles: Synthesis, Supramolecular Assembly with Porphyrin, Intrinsic Peroxidase-like Catalytic Activity and Applications. *Nano Res.* **2011**, *4* (9), 908–920. https://doi.org/10.1007/s12274-011-0147-4.
(54) Righetto, M.; Carraro, F.; Privitera, A.; Marafon, G.; Moretto, A.; Ferrante, C. The Elusive Nature of Carbon Nanodot Fluorescence: An Unconventional Perspective. *J. Phys. Chem. C* **2020**, *124* (40), 22314–22320. https://doi.org/10.1021/acs.jpcc.0c06996.
(55) Neelamraju, B.; Watts, K. E.; Pemberton, J. E.; Ratcliff, E. L. Correlation of Coexistent Charge Transfer States in F_4 TCNQ-Doped P3HT with Microstructure. *J. Phys. Chem. Lett.* **2018**, *9* (23), 6871–6877. https://doi.org/10.1021/acs.jpclett.8b03104.
(56) Soni, N.; Singh, S.; Sharma, S.; Batra, G.; Kaushik, K.; Rao, C.; Verma, N. C.; Mondal, B.; Yadav, A.; Nandi, C. K. Absorption and Emission of Light in Red Emissive Carbon Nanodots. *Chem. Sci.* **2021**, *12* (10), 3615–3626. https://doi.org/10.1039/D0SC05879C.
(57) Singhal, P.; Vats, B. G.; Pulhani, V. Origin of Solvent and Excitation Dependent Emission in Newly Synthesized Amphiphilic Carbon Dots. *Journal of Luminescence* **2022**, *244*, 118742. https://doi.org/10.1016/j.jlumin.2022.118742.
(58) Velusamy, J.; Ramos-Ortiz, G. Na-Doped Carbon Nanodots: Shed Light on the Concentration Modulated Photoluminescence and Two-Photon Absorption Performance. *Colloids and Surfaces A: Physicochemical and Engineering Aspects* **2022**, *634*, 127993. https://doi.org/10.1016/j.colsurfa.2021.127993.
(59) Peterson, J. J.; Werre, M.; Simon, Y. C.; Coughlin, E. B.; Carter, K. R. Carborane-Containing Polyfluorene: *O*- Carborane in the Main Chain. *Macromolecules* **2009**, *42* (22), 8594–8598. https://doi.org/10.1021/ma901703r.
(60) Cook, A. R.; Valášek, M.; Funston, A. M.; Poliakov, P.; Michl, J.; Miller, J. R. *P* - Carborane Conjugation in Radical Anions of Cage–Cage and Cage–Phenyl Compounds. *J. Phys. Chem. A* **2018**, *122* (3), 798–810. https://doi.org/10.1021/acs.jpca.7b10885.
(61) Lu, W.; Do, D. C. H.; Kinjo, R. A Flat Carborane with Multiple Aromaticity beyond Wade–Mingos' Rules. *Nat Commun* **2020**, *11* (1), 3370. https://doi.org/10.1038/s41467-020-17166-9.
(62) Jäkle, F. Advances in the Synthesis of Organoborane Polymers for Optical, Electronic, and Sensory Applications. *Chem. Rev.* **2010**, *110* (7), 3985–4022. https://doi.org/10.1021/cr100026f.

(63) Issa, F.; Kassiou, M.; Rendina, L. M. Boron in Drug Discovery: Carboranes as Unique Pharmacophores in Biologically Active Compounds. *Chem. Rev.* **2011**, *111* (9), 5701–5722. https://doi.org/10.1021/cr2000866.
(64) Kokado, K.; Chujo, Y. Emission via Aggregation of Alternating Polymers with *o* -Carborane and *p* -Phenylene−Ethynylene Sequences. *Macromolecules* **2009**, *42* (5), 1418–1420. https://doi.org/10.1021/ma8027358.
(65) Kokado, K.; Tokoro, Y.; Chujo, Y. Luminescent *m* -Carborane-Based π-Conjugated Polymer. *Macromolecules* **2009**, *42* (8), 2925–2930. https://doi.org/10.1021/ma900174j.
(66) Kokado, K.; Tominaga, M.; Chujo, Y. Aromatic Ring-Fused Carborane-Based Luminescent π-Conjugated Polymers. *Macromol. Rapid Commun.* **2010**, *31* (15), 1389–1394. https://doi.org/10.1002/marc.201000160.
(67) Kokado, K.; Chujo, Y. Multicolor Tuning of Aggregation-Induced Emission through Substituent Variation of Diphenyl- *o* -Carborane. *J. Org. Chem.* **2011**, *76* (1), 316–319. https://doi.org/10.1021/jo101999b.
(68) Yan, J.-F.; Zhu, G.-G.; Yuan, Y.; Lin, C.-X.; Huang, S.-P.; Yuan, Y.-F. Carborane Bridged Ferrocenyl Conjugated Molecules: Synthesis, Structure, Electrochemistry and Photophysical Properties. *New J. Chem.* **2020**, *44* (18), 7569–7576. https://doi.org/10.1039/D0NJ00826E.
(69) Ugrinov, A.; Sevov, S. C. $[Ge_9 Ge_9 Ge_9 Ge_9]^{8-}$: A Linear Tetramer of Nine-Atom Germanium Clusters, a Nanorod. *Inorg. Chem.* **2003**, *42* (19), 5789–5791. https://doi.org/10.1021/ic034677+.
(70) Todorov, I.; Sevov, S. C. Heavy-Metal Aromatic and Conjugated Species: Rings, Oligomers, and Chains of Tin in $Li_{9-x}EuSn_{6+x}$, $Li_{9-x}CaSn_{6+x}$, $Li_5Ca_7Sn_{11}$, $Li_6Eu_5Sn_9$, $LiMgEu_2Sn_3$, and $LiMgSr_2Sn_3$. *Inorg. Chem.* **2005**, *44* (15), 5361–5369. https://doi.org/10.1021/ic050803t.
(71) Neukermans, S.; Janssens, E.; Tanaka, H.; Silverans, R. E.; Lievens, P. Element- and Size-Dependent Electron Delocalization in A u N X + Clusters (X = S c , Ti, V, Cr, Mn, Fe, Co, Ni). *Phys. Rev. Lett.* **2003**, *90* (3), 033401. https://doi.org/10.1103/PhysRevLett.90.033401.
(72) Janssens, E.; Neukermans, S.; Wang, X.; Veldeman, N.; Silverans, R. E.; Lievens, P. Stability Patterns of Transition Metal Doped Silver Clusters: Dopant- and Size-Dependent Electron Delocalization. *Eur. Phys. J. D* **2005**, *34* (1–3), 23–27. https://doi.org/10.1140/epjd/e2005-00106-9.
(73) Walter, M.; Akola, J.; Lopez-Acevedo, O.; Jadzinsky, P. D.; Calero, G.; Ackerson, C. J.; Whetten, R. L.; Grönbeck, H.; Häkkinen, H. A Unified View of Ligand-Protected Gold Clusters as Superatom Complexes. *Proc. Natl. Acad. Sci. U.S.A.* **2008**, *105* (27), 9157–9162. https://doi.org/10.1073/pnas.0801001105.
(74) Grönbeck, H. Correspondence: On the Bonding in Ligand-Protected Gold Clusters. *Nat Commun* **2017**, *8* (1), 1612. https://doi.org/10.1038/s41467-017-01292-y.
(75) Tamaki, R.; Choi, J.; Laine, R. M. A Polyimide Nanocomposite from Octa(Aminophenyl)Silsesquioxane. *Chem. Mater.* **2003**, *15* (3), 793–797. https://doi.org/10.1021/cm020797o.
(76) Choi, J.; Tamaki, R.; Kim, S. G.; Laine, R. M. Organic/Inorganic Imide Nanocomposites from Aminophenylsilsesquioxanes. *Chem. Mater.* **2003**, *15* (17), 3365–3375. https://doi.org/10.1021/cm030286h.

(77) Vij, V.; Haddad, T. S.; Yandek, G. R.; Ramirez, S. M.; Mabry, J. M. Synthesis of Aromatic Polyhedral Oligomeric SilSesquioxane (POSS) Dianilines for Use in High-Temperature Polyimides. *Silicon* **2012**, *4* (4), 267–280. https://doi.org/10.1007/s12633-012-9130-2.
(78) Lee, Andre. Fundamentals of Nano-Structured High-Performance Polyimide Matrix Carbon-Fiber Reinforced Composites, 2011.
(79) Kim, Y.; Koh, K.; Roll, M. F.; Laine, R. M.; Matzger, A. J. Porous Networks Assembled from Octaphenylsilsesquioxane Building Blocks. *Macromolecules* **2010**, *43* (17), 6995–7000. https://doi.org/10.1021/ma101597h.
(80) Laine, R. M.; Roll, M. F. Polyhedral Phenylsilsesquioxanes. *Macromolecules* **2011**, *44* (5), 1073–1109. https://doi.org/10.1021/ma102360t.
(81) Voronkov, M. G.; Lavrent'yev, V. I. Polyhedral Oligosilsesquioxanes and Their Homo Derivatives. In *Inorganic Ring Systems*; Boschke, F. L., Dewar, M. J. S., Dunitz, J. D., Hafner, K., Heilbronner, E., Itô, S., Lehn, J.-M., Niedenzu, K., Raymond, K. N., Rees, C. W., Schäfer, K., Vögtle, F., Wittig, G., Series Eds.; Topics in Current Chemistry; Springer Berlin Heidelberg: Berlin, Heidelberg, 1982; Vol. 102, pp 199–236. https://doi.org/10.1007/3-540-11345-2_12.
(82) Feher, F. J.; Budzichowski, T. A. Syntheses of Highly-Functionalized Polyhedral Oligosilsesquioxanes. *Journal of Organometallic Chemistry* **1989**, *379* (1–2), 33–40. https://doi.org/10.1016/0022-328X(89)80022-1.
(83) Baney, R. H.; Itoh, Maki.; Sakakibara, Akihito.; Suzuki, Toshio. Silsesquioxanes. *Chem. Rev.* **1995**, *95* (5), 1409–1430. https://doi.org/10.1021/cr00037a012.
(84) A. Provatas; J. G. Matisons. Synthesis and Applications of Silsesquioxanes. In *Trends Polym. Sci.*; 1997; Vol. 5, pp 327–322.
(85) Li, G.; Wang, L.; Ni, H.; Pittman Jr., C. U. Polyhedral Oligomeric Silsesquioxane (POSS) Polymers and Copolymers: A Review. *Journal of Inorganic and Organometallic Polymers* **2001**, *11* (3), 123–154. https://doi.org/10.1023/A:1015287910502.
(86) Duchateau, R. Incompletely Condensed Silsesquioxanes: Versatile Tools in Developing Silica-Supported Olefin Polymerization Catalysts. *Chem. Rev.* **2002**, *102* (10), 3525–3542. https://doi.org/10.1021/cr010386b.
(87) Phillips, S. H.; Haddad, T. S.; Tomczak, S. J. Developments in Nanoscience: Polyhedral Oligomeric Silsesquioxane (POSS)-Polymers. *Current Opinion in Solid State and Materials Science* **2004**, *8* (1), 21–29. https://doi.org/10.1016/j.cossms.2004.03.002.
(88) Lickiss, P. D.; Rataboul, F. Fully Condensed Polyhedral Oligosilsesquioxanes (POSS): From Synthesis to Application. In *Advances in Organometallic Chemistry*; Elsevier, 2008; Vol. 57, pp 1–116. https://doi.org/10.1016/S0065-3055(08)00001-4.
(89) Cordes, D. B.; Lickiss, P. D.; Rataboul, F. Recent Developments in the Chemistry of Cubic Polyhedral Oligosilsesquioxanes. *Chem. Rev.* **2010**, *110* (4), 2081–2173. https://doi.org/10.1021/cr900201r.
(90) Wu, J.; Mather, P. T. POSS Polymers: Physical Properties and Biomaterials Applications. *Polymer Reviews* **2009**, *49* (1), 25–63. https://doi.org/10.1080/15583720802656237.
(91) Laine, R. M.; Roll, M. F. Polyhedral Phenylsilsesquioxanes. *Macromolecules* **2011**, *44* (5), 1073–1109. https://doi.org/10.1021/ma102360t.
(92) *Applications of Polyhedral Oligomeric Silsesquioxanes*; Hartmann-Thompson, C., Ed.; Advances in silicon science; Springer: Dordrecht, 2011.

(93) Dudziec, B.; Marciniec, B. Double-Decker Silsesquioxanes: Current Chemistry and Applications. *COC* **2018**, *21* (28). https://doi.org/10.2174/1385272820666151228193728.
(94) Du, Y.; Liu, H. Cage-like Silsesquioxanes-Based Hybrid Materials. *Dalton Trans.* **2020**, *49* (17), 5396–5405. https://doi.org/10.1039/D0DT00587H.
(95) Du, Y.; Liu, H. Triazine-Functionalized Silsesquioxane-Based Hybrid Porous Polymers for Efficient Photocatalytic Degradation of Both Acidic and Basic Dyes under Visible Light. *ChemCatChem* **2021**, *13* (24), 5178–5190. https://doi.org/10.1002/cctc.202101231.
(96) Soldatov, M.; Liu, H. Hybrid Porous Polymers Based on Cage-like Organosiloxanes: Synthesis, Properties and Applications. *Progress in Polymer Science* **2021**, *119*, 101419. https://doi.org/10.1016/j.progpolymsci.2021.101419.
(97) Tamaki, R.; Tanaka, Y.; Asuncion, M. Z.; Choi, J.; Laine, R. M. Octa(Aminophenyl)Silsesquioxane as a Nanoconstruction Site. *J. Am. Chem. Soc.* **2001**, *123* (49), 12416–12417. https://doi.org/10.1021/ja011781m.
(98) Brick, C. M.; Tamaki, R.; Kim, S.-G.; Asuncion, M. Z.; Roll, M.; Nemoto, T.; Ouchi, Y.; Chujo, Y.; Laine, R. M. Spherical, Polyfunctional Molecules Using Poly(Bromophenylsilsesquioxane)s as Nanoconstruction Sites. *Macromolecules* **2005**, *38* (11), 4655–4660. https://doi.org/10.1021/ma0473014.
(99) Brick, C. M.; Ouchi, Y.; Chujo, Y.; Laine, R. M. Robust Polyaromatic Octasilsesquioxanes from Polybromophenylsilsesquioxanes, Br $_\textrmx$ OPS, via Suzuki Coupling. *Macromolecules* **2005**, *38* (11), 4661–4665. https://doi.org/10.1021/ma0501141.
(100) Roll, M. F.; Asuncion, M. Z.; Kampf, J.; Laine, R. M. *Para* -Octaiodophenylsilsesquioxane, [*p* -IC $_6$ H $_4$ SiO $_{1.5}$] $_8$, a Nearly Perfect Nano-Building Block. *ACS Nano* **2008**, *2* (2), 320–326. https://doi.org/10.1021/nn700196d.
(101) Roll, M. F.; Mathur, P.; Takahashi, K.; Kampf, J. W.; Laine, R. M. [PhSiO1.5]8 Promotes Self-Bromination to Produce [o-BrPhSiO1.5]8: Further Bromination Gives Crystalline [2,5-Br2PhSiO1.5]8 with a Density of 2.32 g Cm−3 and a Calculated Refractive Index of 1.7 or the Tetraicosa Bromo Compound [Br3PhSiO1.5]8. *J. Mater. Chem.* **2011**, *21* (30), 11167. https://doi.org/10.1039/c1jm11536g.
(102) Bahrami, M.; Hashemi, H.; Ma, X.; Kieffer, J.; Laine, R. M. Why Do the [PhSiO $_{1.5}$] $_{8,10,12}$ Cages Self-Brominate Primarily in the Ortho Position? Modeling Reveals a Strong Cage Influence on the Mechanism. *Phys. Chem. Chem. Phys.* **2014**, *16* (47), 25760–25764. https://doi.org/10.1039/C4CP03997A.
(103) Roll, M. F.; Kampf, J. W.; Kim, Y.; Yi, E.; Laine, R. M. Nano Building Blocks via Iodination of [PhSiO $_{1.5}$] $_n$, Forming [*p* -I-C $_6$ H $_4$ SiO $_{1.5}$] $_n$ (*n* = 8, 10, 12), and a New Route to High-Surface-Area, Thermally Stable, Microporous Materials via Thermal Elimination of I $_2$. *J. Am. Chem. Soc.* **2010**, *132* (29), 10171–10183. https://doi.org/10.1021/ja102453s.
(104) Burroughes, J. H.; Bradley, D. D. C.; Brown, A. R.; Marks, R. N.; Mackay, K.; Friend, R. H.; Burns, P. L.; Holmes, A. B. Light-Emitting Diodes Based on Conjugated Polymers. *Nature* **1990**, *347* (6293), 539–541. https://doi.org/10.1038/347539a0.
(105) Bazan, G. C.; Miao, Y.-J.; Renak, M. L.; Sun, B. J. Fluorescence Quantum Yield of Poly(*p* -Phenylenevinylene) Prepared via the Paracyclophene Route: Effect of Chain Length and Interchain Contacts. *J. Am. Chem. Soc.* **1996**, *118* (11), 2618–2624. https://doi.org/10.1021/ja953716g.

(106) Laine, R. M.; Sulaiman, S.; Brick, C.; Roll, M.; Tamaki, R.; Asuncion, M. Z.; Neurock, M.; Filhol, J.-S.; Lee, C.-Y.; Zhang, J.; Goodson, T.; Ronchi, M.; Pizzotti, M.; Rand, S. C.; Li, Y. Synthesis and Photophysical Properties of Stilbeneoctasilsesquioxanes. Emission Behavior Coupled with Theoretical Modeling Studies Suggest a 3-D Excited State Involving the Silica Core. *J. Am. Chem. Soc.* **2010**, *132* (11), 3708–3722. https://doi.org/10.1021/ja9087709.

(107) Bassindale, A. R.; Pourny, M.; Taylor, P. G.; Hursthouse, M. B.; Light, M. E. Fluoride-Ion Encapsulation within a Silsesquioxane Cage. *Angew. Chem. Int. Ed.* **2003**, *42* (30), 3488–3490. https://doi.org/10.1002/anie.200351249.

(108) Anderson, S. E.; Bodzin, D. J.; Haddad, T. S.; Boatz, J. A.; Mabry, J. M.; Mitchell, C.; Bowers, M. T. Structural Investigation of Encapsulated Fluoride in Polyhedral Oligomeric Silsesquioxane Cages Using Ion Mobility Mass Spectrometry and Molecular Mechanics. *Chem. Mater.* **2008**, *20* (13), 4299–4309. https://doi.org/10.1021/cm800058z.

(109) Sulaiman, S.; Bhaskar, A.; Zhang, J.; Guda, R.; Goodson, T.; Laine, R. M. Molecules with Perfect Cubic Symmetry as Nanobuilding Blocks for 3-D Assemblies. Elaboration of Octavinylsilsesquioxane. Unusual Luminescence Shifts May Indicate Extended Conjugation Involving the Silsesquioxane Core. *Chem. Mater.* **2008**, *20* (17), 5563–5573. https://doi.org/10.1021/cm801017e.

(110) Sulaiman, S.; Bhaskar, A.; Zhang, J.; Guda, R.; Goodson, T.; Laine, R. M. Molecules with Perfect Cubic Symmetry as Nanobuilding Blocks for 3-D Assemblies. Elaboration of Octavinylsilsesquioxane. Unusual Luminescence Shifts May Indicate Extended Conjugation Involving the Silsesquioxane Core. *Chem. Mater.* **2008**, *20* (17), 5563–5573. https://doi.org/10.1021/cm801017e.

(111) Asuncion, M. Z.; Laine, R. M. Fluoride Rearrangement Reactions of Polyphenyl- and Polyvinylsilsesquioxanes as a Facile Route to Mixed Functional Phenyl, Vinyl T_{10} and T_{12} Silsesquioxanes. *J. Am. Chem. Soc.* **2010**, *132* (11), 3723–3736. https://doi.org/10.1021/ja9087743.

(112) Krug, D. J.; Asuncion, M. Z.; Laine, R. M. Facile Approach to Recycling Highly Cross-Linked Thermoset Silicone Resins under Ambient Conditions. *ACS Omega* **2019**, *4* (2), 3782–3789. https://doi.org/10.1021/acsomega.8b02927.

(113) Furgal, J. C.; Jung, J. H.; Clark, S.; Goodson, T.; Laine, R. M. Beads on a Chain (BoC) Phenylsilsesquioxane (SQ) Polymers via F^- Catalyzed Rearrangements and ADMET or Reverse Heck Cross-Coupling Reactions: Through Chain, Extended Conjugation in 3-D with Potential for Dendronization. *Macromolecules* **2013**, *46* (19), 7591–7604. https://doi.org/10.1021/ma401423f.

(114) Jung, J. H.; Furgal, J. C.; Clark, S.; Schwartz, M.; Chou, K.; Laine, R. M. Beads on a Chain (BoC) Polymers with Model Dendronized Beads. Copolymerization of $[(4\text{-}NH_2C_6H_4SiO_{1.5})_6(IPhSiO_{1.5})_2]$ and $[(4\text{-}CH_3OC_6H_4SiO_{1.5})_6(IPhSiO_{1.5})_2]$ with 1,4-Diethynylbenzene (DEB) Gives Through-Chain, Extended 3-D Conjugation in the Excited State That Is an Average of the Corresponding Homopolymers. *Macromolecules* **2013**, *46* (19), 7580–7590. https://doi.org/10.1021/ma401422t.

(115) Guan, J.; Tomobe, K.; Madu, I.; Goodson, T.; Makhal, K.; Trinh, M. T.; Rand, S. C.; Yodsin, N.; Jungsuttiwong, S.; Laine, R. M. Photophysical Properties of Partially Functionalized Phenylsilsesquioxane: $[RSiO_{1.5}]_7[Me/NPrSiO_{1.5}]$ and $[RSiO_{1.5}]_7[O_{0.5}SiMe_3]_3$ (R = 4-Me/4-CN-Stilbene). Cage-Centered Magnetic Fields Form

under Intense Laser Light. *Macromolecules* **2019**, *52* (11), 4008–4019. https://doi.org/10.1021/acs.macromol.9b00699.

(116) Guan, J.; Tomobe, K.; Madu, I.; Goodson, T.; Makhal, K.; Trinh, M. T.; Rand, S. C.; Yodsin, N.; Jungsuttiwong, S.; Laine, R. M. Photophysical Properties of Functionalized Double Decker Phenylsilsesquioxane Macromonomers: $[PhSiO_{1.5}]_8[OSiMe_2]_2$ and $[PhSiO_{1.5}]_8[O_{0.5}SiMe_3]_4$. Cage-Centered Lowest Unoccupied Molecular Orbitals Form Even When Two Cage Edge Bridges Are Removed, Verified by Modeling and Ultrafast Magnetic Light Scattering Experiments. *Macromolecules* **2019**, *52* (19), 7413–7422. https://doi.org/10.1021/acs.macromol.9b00700.

(117) Chan, K. L.; Sonar, P.; Sellinger, A. Cubic Silsesquioxanes for Use in Solution Processable Organic Light Emitting Diodes (OLED). *J. Mater. Chem.* **2009**, *19* (48), 9103. https://doi.org/10.1039/b909234j.

(118) Sulaiman, S.; Zhang, J.; Goodson, III, T.; Laine, R. M. Synthesis, Characterization and Photophysical Properties of Polyfunctional Phenylsilsesquioxanes: $[O\text{-}RPhSiO_{1.5}]_8$, $[2,5\text{-}R_2PhSiO_{1.5}]_8$, and $[R_3PhSiO_{1.5}]_8$. Compounds with the Highest Number of Functional Units/Unit Volume. *J. Mater. Chem.* **2011**, *21* (30), 11177. https://doi.org/10.1039/c1jm11701g.

(119) Furgal, J. C.; Jung, J. H.; Goodson, T.; Laine, R. M. Analyzing Structure–Photophysical Property Relationships for Isolated T_8, T_{10}, and T_{12} Stilbenevinylsilsesquioxanes. *J. Am. Chem. Soc.* **2013**, *135* (33), 12259–12269. https://doi.org/10.1021/ja4043092.

(120) Guan, J.; Arias, J. J. R.; Tomobe, K.; Ansari, R.; Marques, M. de F. V.; Rebane, A.; Mahbub, S.; Furgal, J. C.; Yodsin, N.; Jungsuttiwong, S.; Hashemi, D.; Kieffer, J.; Laine, R. M. Unconventional Conjugation via $VinylMeSi(O^-)_2$ Siloxane Bridges May Imbue Semiconducting Properties in $[Vinyl(Me)SiO(PhSiO_{1.5})_8OSi(Me)Vinyl\text{-}Ar]$ Double-Decker Copolymers. *ACS Appl. Polym. Mater.* **2020**, acsapm.0c00591. https://doi.org/10.1021/acsapm.0c00591.

(121) Guan, J.; Sun, Z.; Ansari, R.; Liu, Y.; Endo, A.; Unno, M.; Ouali, A.; Mahbub, S.; Furgal, J. C.; Yodsin, N.; Jungsuttiwong, S.; Hashemi, D.; Kieffer, J.; Laine, R. M. Conjugated Copolymers That Shouldn't Be. *Angew. Chem. Int. Ed.* **2021**, *60* (20), 11115–11119. https://doi.org/10.1002/anie.202014932.

(122) Méndez, H.; Heimel, G.; Winkler, S.; Frisch, J.; Opitz, A.; Sauer, K.; Wegner, B.; Oehzelt, M.; Röthel, C.; Duhm, S.; Többens, D.; Koch, N.; Salzmann, I. Charge-Transfer Crystallites as Molecular Electrical Dopants. *Nat Commun* **2015**, *6* (1), 8560. https://doi.org/10.1038/ncomms9560.

(123) Jacobs, I. E.; Moulé, A. J. Controlling Molecular Doping in Organic Semiconductors. *Adv. Mater.* **2017**, *29* (42), 1703063. https://doi.org/10.1002/adma.201703063.

(124) Jun guan; Zijing Zhang; Ramen Ansari; John Kieffer; Nuttapon Yodsin; Siriporn Jungsuttiwong; Richard M. Laine. Further Proof of Unconventional Conjugation via Disiloxane Bonds. Double Decker Silses-Quioxane [VinylM $Si(O_{0.5})_2(PhSiO_{1.5})_8(O_{0.5})_2SiMevinyl$] Derived Alternating Terpolymers Give Excited-State Conjugation Averaging That of the Corresponding Co-Polymers.

(125) Liu, Y.; Takeda, N.; Ouali, A.; Unno, M. Synthesis, Characterization, and Functionalization of Tetrafunctional Double-Decker Siloxanes. *Inorg. Chem.* **2019**, *58* (7), 4093–4098. https://doi.org/10.1021/acs.inorgchem.9b00416.

(126) Guan, J.; Arias, J. J. R.; Tomobe, K.; Ansari, R.; Marques, M. de F. V.; Rebane, A.; Mahbub, S.; Furgal, J. C.; Yodsin, N.; Jungsuttiwong, S.; Hashemi, D.; Kieffer, J.; Laine,

R. M. Unconventional Conjugation via VinylMeSi(O−)$_2$ Siloxane Bridges May Imbue Semiconducting Properties in [Vinyl(Me)SiO(PhSiO$_{1.5}$)$_8$OSi(Me)Vinyl-Ar] Double-Decker Copolymers. *ACS Appl. Polym. Mater.* **2020**, *2* (9), 3894–3907. https://doi.org/10.1021/acsapm.0c00591.

(127) Aleksander Rebane. Annual Report to NSF for Chem. Award 2103602.